Neuron

Article

Meningeal neutrophil immune signaling influences behavioral adaptation following threat

Graphical abstract

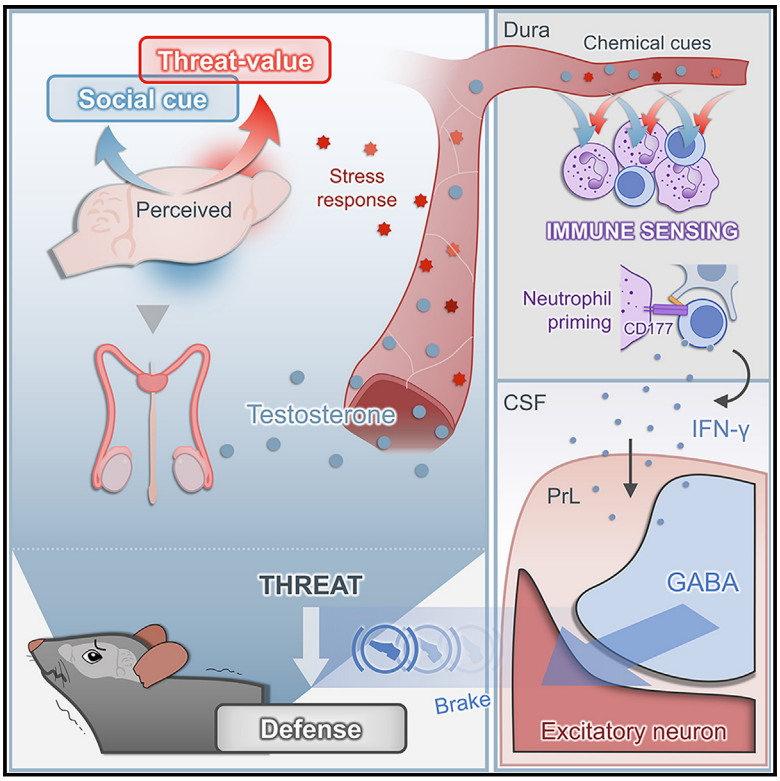

Highlights

- Socially cued threats prime meningeal neutrophils (MNs) in males
- The priming of MNs suppresses behavioral threat responses
- MNs acquire the CD177 signal that triggers IFN-γ-mediated GABAergic inhibition
- Androgen responsiveness directs meningeal immune signaling when threatened

Authors

Bin Wu, Ling Meng, Yan Zhao, ..., Yayan Pang, Chunguang Ren, Zhifang Dong

Correspondence

chunguangren@cqmu.edu.cn (C.R.), zfdong@cqmu.edu.cn (Z.D.)

In brief

Wu et al. demonstrate how neutrophils, located within the protective layers of the brain, respond to social threats and modulate psychological processes. This process is governed by testosterone in a context-dependent manner and is executed by neutrophil-mediated meningeal immunity, which impedes threat-related neural activity via IFN-γ-GABAergic signaling axis.

Wu et al., 2025, Neuron *113*, 1–17
January 22, 2025
https://doi.org/10.1016/j.neuron.2024.10.018

CellPress

Please cite this article in press as: Wu et al., Meningeal neutrophil immune signaling influences behavioral adaptation following threat, Neuron (2024), https://doi.org/10.1016/j.neuron.2024.10.018

Neuron

CellPress

Article

Meningeal neutrophil immune signaling influences behavioral adaptation following threat

Bin Wu,[1,4] Ling Meng,[2,3,4] Yan Zhao,[3] Junjie Li,[1] Qiuyun Tian,[1] Yayan Pang,[1] Chunguang Ren,[2,*] and Zhifang Dong[1,5,*]
[1]Growth, Development, and Mental Health of Children and Adolescence Center, Pediatric Research Institute, Ministry of Education Key Laboratory of Child Development and Disorders, National Clinical Research Center for Child Health and Disorders, Chongqing Key Laboratory of Child Neurodevelopment and Cognitive Disorders, Children's Hospital of Chongqing Medical University, Chongqing, China
[2]Laboratory of Developmental Biology, Department of Cell Biology and Genetics, School of Basic Medical Sciences, Chongqing Medical University, Chongqing, China
[3]Department of Respiratory Medicine, The Second Affiliated Hospital of Chongqing Medical University, Chongqing, China
[4]These authors contributed equally
[5]Lead contact
*Correspondence: chunguangren@cqmu.edu.cn (C.R.), zfdong@cqmu.edu.cn (Z.D.)
https://doi.org/10.1016/j.neuron.2024.10.018

SUMMARY

Social creatures must attend to threat signals from conspecifics and respond appropriately, both behaviorally and physiologically. In this work, we show in mice a threat-sensitive immune mechanism that orchestrates psychological processes and is amenable to social modulation. Repeated encounters with socially cued threats triggered meningeal neutrophil (MN) priming preferentially in males. MN activity was correlated with attenuated defensive responses to cues. Canonical neutrophil-specific activation marker CD177 was upregulated after social threat cueing, and its genetic ablation abrogated male behavioral phenotypes. CD177 signals favored meningeal T helper (Th)1-like immune bias, which blunted neural response to threatening stimuli by enhancing intrinsic GABAergic inhibition within the prelimbic cortex via interferon-gamma (IFN-γ). MN signaling was sensitized by negative emotional states and governed by socially dependent androgen release. This male-biased hormone/neutrophil regulatory axis is seemingly conserved in humans. Our findings provide insights into how immune responses influence behavioral threat responses, suggesting a possible neuroimmune basis of emotional regulation.

INTRODUCTION

Danger perception, a primitive brain function, triggers short-term bodily adjustments that enable adaptation to external stimuli, promoting organisms to survive and thrive.[1–4] The detection of stimuli capable of eliciting threat responses relies on innate programming or past experiences. In contemporary settings, neutral cues can signal threat, a cognitive process that occurs when interacting with social environments. Such cues contain a conditioned warning value that is sufficient to trigger defense based on learned associations.[5] The initial triggering of defensive responses is pre-encoded, but with proximate experiences and learning, emotional states or behaviors are modified.

Internally induced physiological responses to stimuli can modulate emotional and behavioral expressions.[3,6,7] The immune system, extending beyond its conventional role in host defense, is thought to maintain homeostasis throughout the body.[8] Overwhelming evidence indicates a conserved hematological response to stressors across vertebrates[9]: elevated neutrophils, the predominant leukocytes in humans. A recent study also shows acute stress can transcriptionally reshape neutrophils.[10] However, the causal impact of neutrophil activity on behavioral states remains largely unexplored. Neutrophils exhibit phenotypic plasticity, enabling them to respond sensitively to changing internal milieu.[11] They express numerous immune receptors, enabling inter-immune cell communication and transmitting and amplifying initial immune signals.[12–14] Further, the meninges constitute the immunologically active tissue closest to the brain. Meningeal immune cells sense the daily oscillations of peripheral blood and cerebrospinal fluid (CSF) to support brain homeostasis.[15] Identification of the immune landscape reveals a dense neutrophil population at the skull-meningeal interface.[16–18] Given these advances, we hypothesized that meningeal neutrophils (MNs) may function as sensors for external threats, instantly signaling the brain.

Social cue (SC) processing is more complex than isolated sensory cues,[19] involving the integration of multiple sensory modalities and neuroendocrine responses related to sexual information. The human immune system is highly sensitive to features of the social environment, with socially relevant acute psychological challenges eliciting stronger pro-inflammatory responses.[20] Social variables and stimulation nature may therefore

Please cite this article in press as: Wu et al., Meningeal neutrophil immune signaling influences behavioral adaptation following threat, Neuron (2024), https://doi.org/10.1016/j.neuron.2024.10.018

be decisive. In this study, we explored whether a neuro-immune circuit at the meningeal-brain interface could integrate external signals to regulate behavior, underlying homeostatic control of emotional states in social contexts.

RESULTS

Sex-specific MN priming after social threat cueing

Behavioral threat responses evoked by SCs may arise from negative social experiences, manifested as conspecific avoidance. The mice underwent social fear (threat) conditioning (SFC) to successfully link SCs with defensive responses (hereafter, SFC+ mice) (Figure S1A). SFC+ mice exhibited strong conspecific avoidance in three-chamber social approach tests, compared with control mice receiving only foot shocks (Figure 1A). However, SFC+ mice showed normal innate avoidance behaviors (Figure S1B), suggesting that SFC did not affect general threat responses.

We next investigated whether exposure to threat-predicting SCs affects MN states in SFC+ mice. 1 day post-conditioning, SFC+ mice were exposed to an unfamiliar conspecific. SFC+ mice received a total of five SC presentations (Figure 1B). Degranulation is an immediate change of neutrophils upon stimulation and can be characterized by increased membrane presentation of internalized antigens.[21,22] Flow cytometry revealed significantly increased surface molecules on MNs in SFC+ males compared with controls (Figures 1C and 1D). These effects were absent in females (Figure 1D) and unconditioned males (Figure S1D). In contrast to exposure to SCs, the levels of surface molecules on MNs did not increase after exposure to threat-predicting inanimate objects or acoustic stimuli (Figures S1E–S1H), despite both non-SCs eliciting strong defensive behaviors (Figure S1I). This suggests MN responses depend on the social nature of the cues. SC-induced upregulation of neutrophil surface molecules was also observed in blood (Figure S1J), indicating consistent responsiveness to threat-predicting SCs in both MNs and circulating neutrophils.

Without trauma or infection, the upregulation of MN surface markers likely indicates a primed state rather than full activation.[23] Increased reactive oxygen species (ROS)-generating capacity and longevity are characteristic of neutrophil priming.[23] The MNs isolated from male SFC+ mice after exposure to SCs exhibited stronger respiratory burst potentials upon phorbol 12-myristate 13-acetate (PMA) stimulation (Figures 1E–1G). These MNs also exhibited a higher proportion of live cells when challenged by lipopolysaccharide (LPS), as evidenced by annexin V and 7-amino-actinomycin D (7-AAD) double-negative gating analysis, indicating a pro-survival phenotype (Figures 1H and 1I). To further confirm the sex differences in MN state following social threat cueing, we performed RNA sequencing (RNA-seq) in MNs of male and female SFC+ mice after exposure and identified 194 differentially expressed genes (DEGs) (Figure 1J; Table S1). Gene Ontology (GO) analysis of 125 upregulated DEGs revealed that crucial immune-related pathways were enriched in male MNs (Figure 1K). All of these GO terms primarily consist of genes associated with innate immune response, antimicrobial response, leukocyte chemotaxis/migration, positive regulation of T cell differentiation, and response to interferon-gamma (IFN-γ). Taken together, these data suggest a sex-specific neutrophil response to socially cued threat, occurring in circulation or at the CNS boundary, which may serve as an adaptive process promoting host defenses.

Temporary alteration of threat reactivity emerges with MN activity

Repeated threat exposure facilitates adaptation of threat responses, leading to extinction or habituation.[24,25] 1 day post-exposure, both male and female SFC+ mice maintained strong avoidance to SCs: they spent most of test time in chambers without conspecifics (Figure S2A). Within 1–3 h post-exposure (Figure 2A), male SFC+ mice showed reduced cue-evoked avoidance: they spent less time in the non-social chamber and more time with conspecifics compared with females or unexposed males (Figures 2B–2E). This suggests that despite being insufficient to induce new learning interfering with threat memory, SC exposure facilitates short-term adaptation in males. Interestingly, the attenuated behavioral response in males can persist for at least a week (Figures 2F–2J). This long-term effect benefits from SC re-exposure during post-testing, as SFC+ males failed to recover from social avoidance when the social target was removed (Figure S2B). Indeed, this result conceptually seems to support previous observations that recall immediately after exposure promotes fear extinction.[26]

To determine if exposure-induced suppression of cue-evoked responses reflected altered general state, we used the open field test (OFT), the elevated plus maze (EPM), and the predator odor exposure (POE) to assess the effects of exposure on anxiety-related innate avoidance behaviors in SFC+ mice. After exposure to SCs, male SFC+ mice showed increased time in EPM open arms and reduced avoidance of 2-methyl-2-thiazoline (2-MT) odor sources, while females exhibited no changes (Figure S2C). Thus, experiencing the socially cued threats appears to blunt behavioral responses to generalized threatening stimuli in males.

Neutrophil priming is reversible, returning to quiescence upon removal of environmental factors. In male SFC+ mice, MN surface molecule levels remained elevated for 3 h post-SC exposure before decreasing (Figure S2D), seemingly consistent with the temporal dynamics of behavioral effects. To test whether short-term MN activity contributed to male-specific behavioral outcomes, we pre-depleted MNs using the antibodies against Ly6G (Figure 2K). We verified that anti-Ly6G treatment partially abolished murine dural neutrophils (Figure 2L). After repeated exposure to SCs, anti-Ly6G-treated male SFC+ mice showed increased avoidance of conspecifics compared with controls, despite no difference in non-social chamber time (Figures 2M and 2N). In females, the anti-Ly6G treatment did not affect post-exposure behavioral parameters (Figure S2E). Granulocyte-macrophage colony-stimulating factor (GM-CSF) positively regulates neutrophil priming and degranulation.[27,28] We next tested if GM-CSF-induced MN priming alters the response to SCs in female SFC+ mice. Transcranial dural GM-CSF delivery (Figure 2O) upregulated CD11b and CD177 levels on MNs (Figure 2P) and increased their respiratory burst capacity *in vitro* (Figure S2F), indicating MN priming. Post-exposure GM-CSF injection reduced non-social zone time and increased conspecific

Please cite this article in press as: Wu et al., Meningeal neutrophil immune signaling influences behavioral adaptation following threat, Neuron (2024), https://doi.org/10.1016/j.neuron.2024.10.018

CellPress

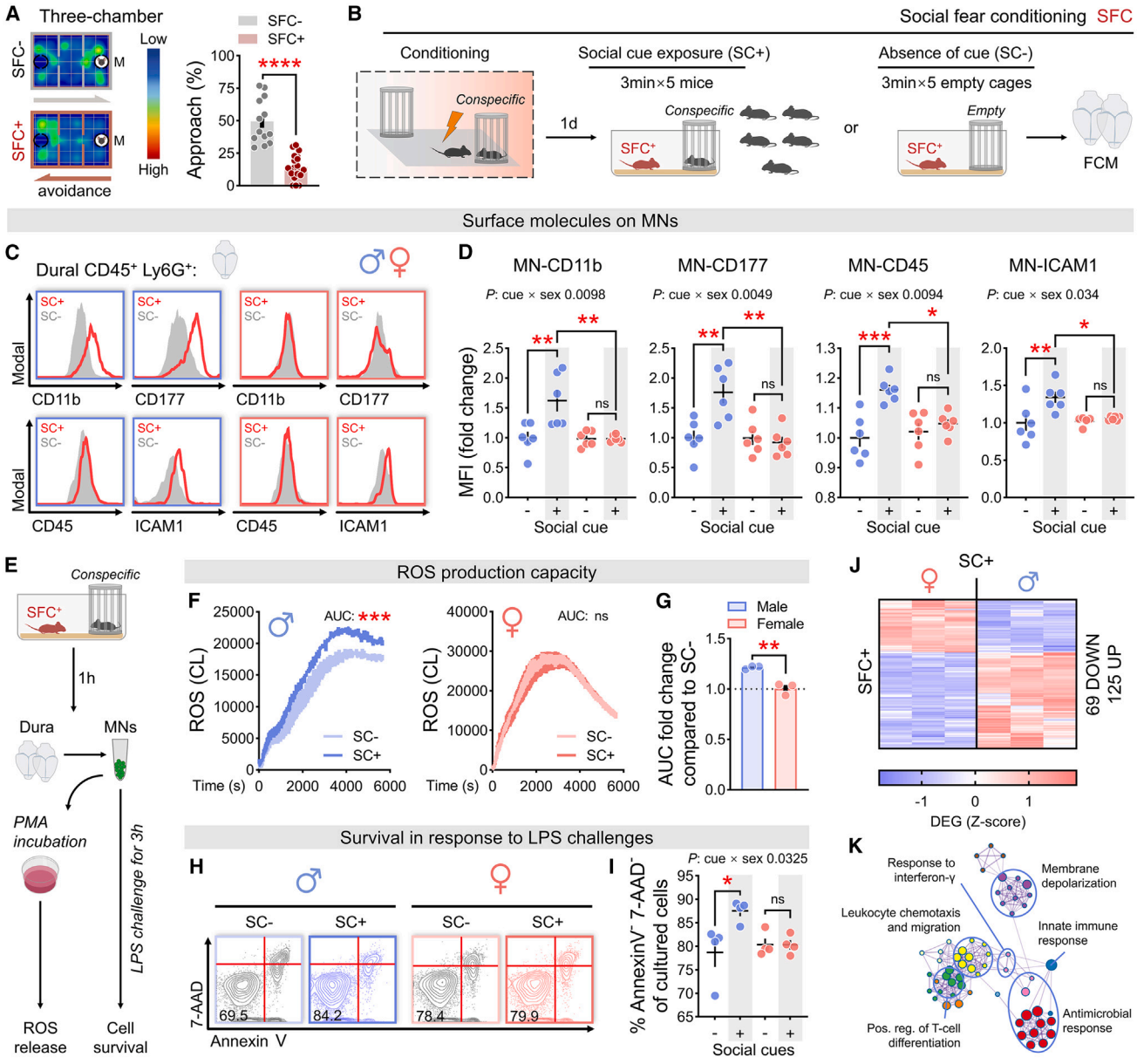

Figure 1. Sex-specific MN priming after social threat cueing

(A) Average heatmaps showing location and time and relative time spent in the social chamber in SFC− and SFC+ mice.

(B) Schematic of the SFC paradigm and socially cued threat exposure.

(C and D) Male and female SFC+ mice were repeatedly exposed to conspecifics or empty cups, and their MN surface phenotypes were analyzed 1 h later by flow cytometry. Representative histograms (C) and relative mean fluorescence intensity (MFI) changes (D) of CD11b, CD177, CD45, and ICAM1 levels on MNs, gated on $CD45^+$ $Ly6G^+$ cells.

(E) Schematic of functional analysis of isolated MNs after exposure to SCs.

(F) ROS generation in MNs from male and female SFC+ mice after exposure to SCs or absence thereof, measured by luminol-dependent chemiluminescence (CL) (meninges were pooled from 2 mice, $n = 6$ per group).

(G) Comparison of the relative amplitude of change in area under the curve (AUC) between male and female in (F).

(H and I) Cell survival in MNs from male and female SFC+ mice after exposure to SCs or absence thereof, measured using cytometry analysis of annexin V/7-AAD-stained cells and the quantitative analysis of % of living cells (meninges were pooled from 2 mice, $n = 8$ per group).

(J) Significant DEGs (fold change > 2, $p < 0.05$) after RNA-seq analysis in MNs from male and female SFC+ mice after exposure to SCs or absence thereof (meninges were pooled from 2 mice, $n = 6$ per group).

(K) GO enrichment map for upregulated DEGs (male vs. female) in (J), generated by Metascape ($p < 0.01$). Blue symbols, males; pink symbols, females. Dots represent individual mice (D) or independent experiments.

(G and I). ns $p > 0.05$, *$p < 0.05$, **$p < 0.01$, ***$p < 0.001$.

See also Figure S1.

Please cite this article in press as: Wu et al., Meningeal neutrophil immune signaling influences behavioral adaptation following threat, Neuron (2024), https://doi.org/10.1016/j.neuron.2024.10.018

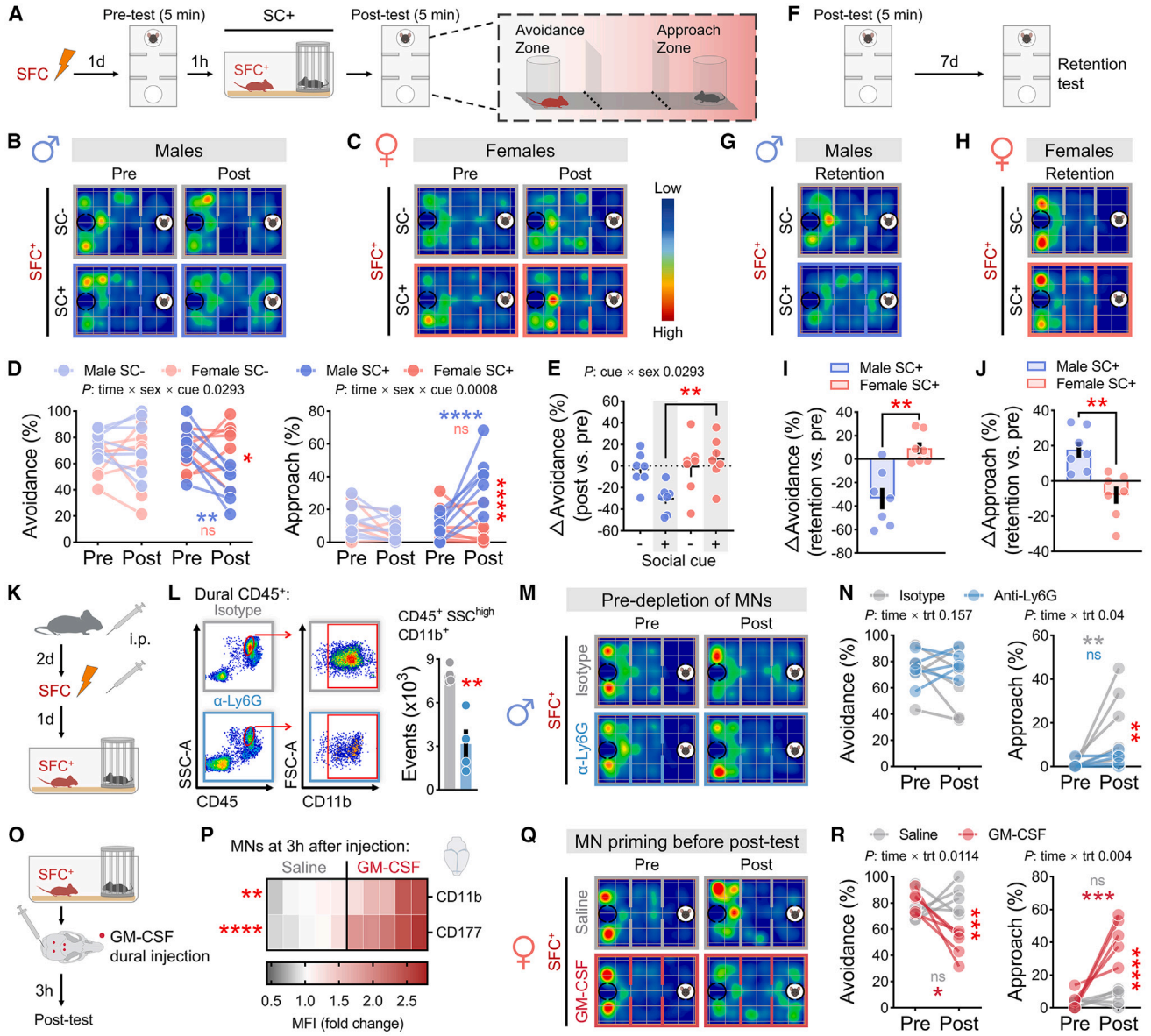

Figure 2. Temporary alteration of threat reactivity emerges with MN activity

(A) Schematic of the social approach test (SAT) before and after exposure session.

(B) Average heatmaps showing location and time during SATs in male SFC+ mice before and after exposure to SCs or absence thereof.

(C) Same as (B), but for females.

(D) Changes in the relative time spent on social avoidance and approach between male and female SFC+ mice after exposure to SCs or absence thereof.

(E) Comparison of changed avoidance responses to SCs.

(F) Schematic of a retention test for social avoidance responses.

(G) Average heatmaps showing location and time during retention tests in male SFC+ mice before and after exposure to SCs or absence thereof.

(H) Same as (G), but for females.

(I and J) Changes in the relative time spent on social avoidance (I) and approach (J) in male and female SFC+ mice during retention tests relative to prior to SC exposure.

(K) Schematic of MN depletion *in vivo* using anti-Ly6G.

(L) MN depletion efficiency with anti-Ly6G measured by flow cytometry.

(M) Average heatmaps showing location and time during SATs in anti-Ly6G- and isotype-treated male SFC+ mice before and after exposure to SCs.

(N) Changes in the relative time spent on social avoidance and approach between anti-Ly6G- and isotype-treated male SFC+ mice after exposure to SCs.

(O) Schematic of inducing MN priming by GM-CSF dural injection.

(P) Heatmap showing the relative MFI changes of CD11b and CD177 on MNs 3 h after GM-CSF injection compared with saline injection.

(legend continued on next page)

Please cite this article in press as: Wu et al., Meningeal neutrophil immune signaling influences behavioral adaptation following threat, Neuron (2024), https://doi.org/10.1016/j.neuron.2024.10.018

interaction in female SFC+ mice, while saline-treated females maintained strong avoidance (Figures 2Q and 2R). In males, GM-CSF slightly reduced avoidance zone time, though not significantly (Figure S2G). Additionally, MN pre-depletion prevented sociability restoration in males, while GM-CSF-mediated MN priming promoted long-term adaptation to cue-evoked avoidance in females (Figures S2H and S2I). Collectively, these data suggest that MN activity modulates behavioral responses to threat-related cues, potentially by attenuating internal arousal or emotional states.

Neutrophil-specific surface signals restrict prefrontal activity under threat

Neutrophils respond to stress through degranulation, rapidly expanding cell membrane proteins, and supporting the microbicidal effector spectrum. Without actual infection, surface protein induction is one of the few terminal events. Secretory vesicles (SVs) are readily mobilized in response to minimal stimulation.[21,22] A previous proteomic study identified 33 conventional membrane-localized proteins that co-present in both neutrophil SV membrane and plasma membrane fractions,[29] associated with cell adhesion and migration (Table S2). These proteins include CD177, a neutrophil-specific surface antigen.[30] Our analysis revealed that surface CD177, as a canonical neutrophil activation marker for infection, was highly induced after SC exposure (Figure 1C). Prominently, surface CD177 has recently been identified as a potent neutrophil effector protein curbing infection.[31] Given this remarkable negative feedback role of CD177 in pathogen threat response, we asked whether a CD177-mediated signal could modulate behavioral responses to psychological threats.

Cd177 ablation in mice cannot affect neutrophil function[32] or baseline MN frequency (Figure S3A), despite reported decreases in peripheral neutrophils. Pre-exposure, male SFC+ Cd177-deficient and wild-type (WT) littermates showed similar social avoidance (Figures 3A and 3B). Post-exposure, male SFC+ Cd177-deficient mice spent less time in social zones and more in non-social zones compared with littermates (Figures 3A and 3B), failing to recover from cue-evoked social avoidance (Figure S3B). *Cd177* ablation also prevented the inhibitory effects of SC exposure on the defensive response to EPM or POE in male SFC+ mice (Figure 3C).

To further investigate the role of CD177 specific to meningeal immune niche, we colonized WT neutrophils in the dura of Cd177-deficient mice. As cranial bone marrow (BM) is a major source of dural myeloid cells,[33] we carried out a calvarial transplantation experiment. The caudal region of the skull harbored a large hematopoietic niche. A WT-cranial bone flap was transplanted onto the skull window of Cd177-deficient mice (Figure 3D). Colonization of the WT-bone flap resulted in increased frequency of $CD177^+$ cells in MNs from Cd177-deficient mice (Figure 3E). Male SFC+ Cd177-deficient mice with WT-bone flaps showed reduced cue-evoked social avoidance post-exposure compared with knockout (KO)-flap recipients (Figures 3F and S3C). As a complementary technique,[34] head-irradiated BM transplantation of WT-BM cells into Cd177-deficient mice increased donor-derived $CD177^+$ dural neutrophils (Figures S3D and S3E) and reduced cue-evoked behavioral threat responses after SC exposure, particularly in social approach (Figure S3F). To further validate CD177 as a mediator between MN activity and behavioral outcomes, we repeated the dural injections of GM-CSF in female SFC+ Cd177-deficient mice. GM-CSF reduced post-exposure avoidance responses in WT littermates but not in Cd177-deficient mice (Figures S3G and S3H).

Superficial neocortical regions beneath the dura mater are preferred for contacting macromolecules in the CSF.[35] The prelimbic cortex (PrL) in the dorsomedial prefrontal cortex (dmPFC) regulates subcortical responses to threats and evaluates stimuli based on context or prior knowledge. PrL disinhibition is linked to fear/anxiety.[36–38] We investigated whether MN activity modulates behavior by altering PrL neuronal reactivity. We first recorded the activities of PrL layer II/III excitatory neurons in male SFC+ mice when witnessing conspecifics before and after repeated SC exposure. A gene-encoding calcium sensor, GCaMP6s, was expressed in PrL projection neurons (PNs) of SFC+ mice (Figure 3H). Male SFC+ mice underwent a 1-min SC recall before and after exposure (day 2) (Figures 3I and 3K). In both trials, bulk changes in GCaMP6s fluorescence in PrL-PNs were monitored using fiber photometry. SFC+ WT littermates without SC exposure showed consistent induced GCaMP6s response in both cued recall tests, indicating that the inter-trial interval did not affect the potential of these neurons to respond to conspecific cues (Figures S3I and S3J). By contrast, SC exposure was associated with reduced GCaMP6s fluorescence in subsequent recall (Figure 3L). Cd177-deficient mice lacked this inhibitory response, instead showing a trend toward increased GCaMP6s fluorescence (Figures 3M and 3N).

We hypothesized that blunted PrL-PN reactivity stemmed from diminished response to general negative stimuli, not specific habituation to conditioned cues. To test this, we recorded PrL-PN GCaMP6s responses to POE in SFC+ mice post-SC exposure (Figures 3J and 3O). WT SFC+ mice showed significantly attenuated 2-MT-evoked GCaMP6s responses after exposure (Figure 3P), an effect impaired in Cd177-deficient mice (Figures 2Q and 3R). Control SFC+ mice without cue exposure maintained consistent fluorescence induction of GCaMP6s between tests (Figures S3K and S3L). Collectively, these findings indicate that CD177, as a socially threat-sensitive immune signal, may be involved in regulating PrL activity.

CD177 orchestrates IFN-γ-mediated prefrontal inhibition

Given that CD177 lacks intracellular domains and direct intracellular signaling cascades due to its glycosylphosphatidylinositol anchoring property, we turned to addressing the tantalizing

(Q) Same as (M), but for GM-CSF- and saline-treated female SFC+ mice.

(R) Same as (N), but for GM-CSF- and saline-treated female SFC+ mice. Blue symbols, males; pink symbols, females. Dots represent individual mice. ns $p > 0.05$, $^*p < 0.05$, $^{**}p < 0.01$, $^{***}p < 0.001$, $^{****}p < 0.0001$.

See also Figure S2.

Please cite this article in press as: Wu et al., Meningeal neutrophil immune signaling influences behavioral adaptation following threat, Neuron (2024), https://doi.org/10.1016/j.neuron.2024.10.018

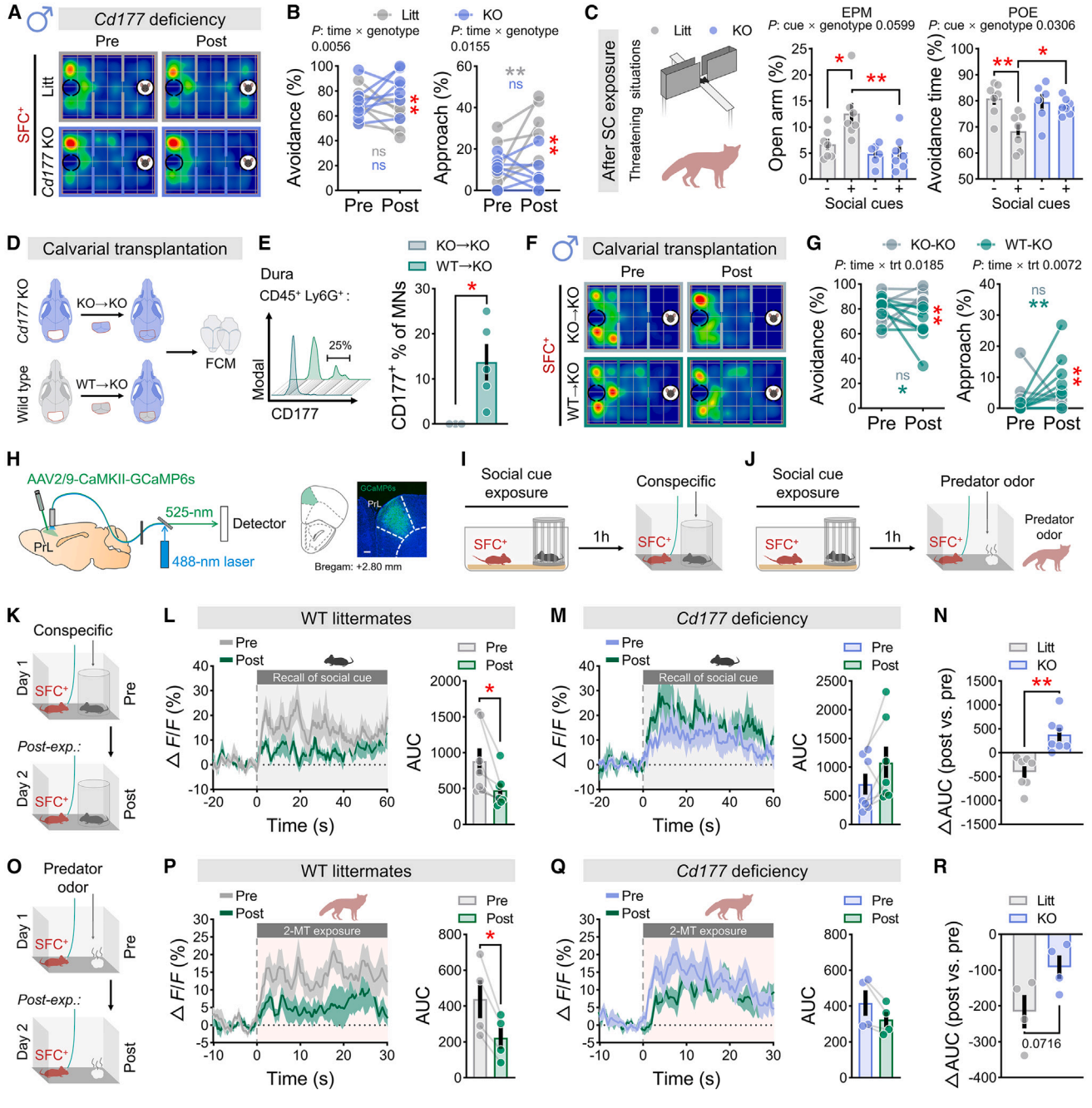

Figure 3. Neutrophil-specific surface signals restrict prefrontal activity under threat

(A) Average heatmaps showing location and time during SATs in male SFC+ Cd177-deficient mice and their littermates before and after exposure to SCs.

(B) Changes in the relative time spent on social avoidance and approach between male SFC+ Cd177-deficient mice and their littermates after exposure to SCs.

(C) EPM- and POE-evoked avoidance behavior in male SFC+ Cd177-deficient mice and their littermates after exposure to SCs or absence thereof.

(D) Schematic of calvaria flap transplantation.

(E) Representative histogram and quantification of $CD177^+$ MNs from Cd177-deficient mice 7 days after calvaria flap transplantation, gated on $CD45^+$ $Ly6G^+$ cells.

(F and G) Same as (A) and (B), but for male SFC+ mice transplanted with $CD177^+$ or $CD177^-$ calvaria flaps.

(H) Schematic and representative image of AAV-dependent expression of GCaMP6s in the PrL of a mouse to monitor PrL excitatory neuronal activity via fiber photometry. Scale bar, 200 μm.

(I and J) Schematic of cue recall (I) and POE (J) tests after socially cued threat experiences.

(K) Schematic of the test of GCaMP6s responses to conspecific in SFC+ mice before and after social exposure.

(legend continued on next page)

Please cite this article in press as: Wu et al., Meningeal neutrophil immune signaling influences behavioral adaptation following threat, Neuron (2024), https://doi.org/10.1016/j.neuron.2024.10.018

possibility that CD177 might function to modulate the immune microenvironment in the dura mater. The upregulated DEGs in male MNs post-exposure showed a strong correlation with T cell differentiation regulation (Figure 1K). This observation prompted us to investigate potential alterations in meningeal adaptive immunity.

Meningeal T cell-derived IFN-γ and interleukin (IL)-17A can modulate mPFC electrochemical signals.[39,40] We first examined the effect of physiological loss of CD177 on cytokine-producing meningeal T cells. Flow cytometry analysis showed a modest decrease in the percentage of IFN-γ-producing $CD3^+$ T cells in the dura of Cd177-deficient mice but did not alter the potential for cell-based IFN-γ production (Figure S4A). *Cd177* ablation had no significant effect on meningeal IL-17A-producing $CD3^+$ T cells (Figure S4A). Neutrophils have previously been reported to regulate natural killer (NK) cell homeostasis.[41] However, minimal IFN-γ^+ cells were detected in meningeal CD3-negative lymphocyte population (Figure S4B).

We further hypothesized that MN CD177 upregulation in response to socially cued threats would promote IFN-γ production by meningeal T cells. After SC exposure, male dural meninges showed increased IFN-γ-producing $CD3^+$ T cells but not IL-17A-producing $CD3^+$ T cells (Figures 4A and 4B). *Cd177* deficiency eliminated this effect (Figure 4B). Female SFC+ mice, whose MN surface phenotype was unaffected by cue exposure (Figure 1D), showed no change in meningeal $CD3^+$ IFN-γ^+ T cells (Figure S4C). We also analyzed the dura mater of Cd177-deficient mice transplanted with WT-cranial bone flaps and observed a relative increase in the frequency of IFN-γ-producing T cells (Figure S4D). Mice receiving WT-BM cells after SC exposure also showed higher frequency of IFN-γ-producing $CD3^+$ T cells in dura mater (Figure S4E), further supporting meningeal induction of IFN-γ by CD177.

The dural sinuses represent immune hubs for antigen-presenting cell (APC)-T cell interactions at steady state.[42] Without additional stimulation, contact culture of mouse $CD177^+$ neutrophils with a mixture of APCs and naive $CD3^+$ T cells induced a significant increase in the frequency of IFN-γ-producing $CD3^+$ T cells (Figure S4F). Sequestration of neutrophils into compartments completely abolished this effect (Figure S4F). It can be inferred that CD177-induced T helper (Th)1-like responses involve physical interactions within the meninges, consistent with the properties of CD177 as a membrane-anchored protein.

IFN-γ is a potent regulator of inhibitory neurotransmission.[43] To examine whether lack of CD177-IFN-γ signaling would affect inhibitory transmission in the PrL, we first recorded minute inhibitory postsynaptic currents (mIPSCs) in PrL pyramidal neurons from male SFC+ littermates and Cd177-deficient mice after SC exposure. WT mice showed increased mIPSC frequency but not amplitude in PrL pyramidal neurons after exposure (Figure 4C). This effect was absent in Cd177-deficient mice (Figure 4C). To further strengthen this observation, we extracted dmPFC synaptic proteins from SFC+ mice at 1 h after exposure. Synaptic protein analysis revealed cue exposure-induced upregulation of inhibitory synaptic markers glutamic acid decarboxylase (GAD) and gephyrin in dmPFC, blocked by *Cd177* ablation (Figure 4D). We next sought to determine whether IFN-γ neutralization in CSF would reproduce the effects caused by *Cd177* ablation. The αIFN-γ neutralizing antibody and isotype controls were injected into the cisterna magna of WT SFC+ mice 3 h before exposure. Treatment with αIFN-γ neutralizing antibody significantly downregulated synaptic GAD and gephyrin levels compared with isotype controls (Figure 4E), suggesting that IFN-γ may mediate the recruitment of GABAergic signals in PrL after social threat cueing. Notably, these data are consistent with the recent demonstration that IFN-γ acts presynaptically to enhance inhibitory tone.[44,45]

In line, we found that pre-treatment with αIFN-γ neutralizing antibody but not isotype control prevented the blunting of PrL excitatory neuronal reactivity elicited by exposure: SFC+ mice treated with αIFN-γ neutralizing antibody showed highly evoked PrL GCaMP6s responses during the presentation of conspecific cues (Figures 4F–4I) or predator odor cues (Figures 4J–4M) in both pre- and post-exposure tests.

IFN-γ-driven suppression of threat-motivated behavior requires PrL^{Gad1} neurons

To determine whether meningeal IFN-γ signaling and prefrontal inhibitory tone after socially cued threats orchestrate behavioral outputs, we bilaterally injected excitatory "designer receptors exclusively activated by designer drugs" (DREADD) AAVs or control AAVs expressing mCherry under the control of Gad1 promoter into the PrL of WT male mice (Figures 5A and 5B). We pre-injected αIFN-γ neutralizing antibody or isotype controls into the cisterna magna of AAV-injected SFC+ mice, followed by the DREADD ligand clozapine N-oxide (CNO) administration after exposure (Figure 5C). CNO-activated GABAergic neurons within the PrL (hereafter, PrL^{Gad1} neurons) in DREADD-expressing (hM3D(Gq)) mice (Figures S5A and S5B). Male SFC+ mice treated with αIFN-γ neutralizing antibody retained a strong avoidance response to social situations (Figures 5D and 5E), reduced open-arm exploration (Figures 5F and S5C), and increased odor-evoked avoidance (Figure 5G) after SC exposure. Critically, chemogenetically activating PrL^{Gad1} neurons in SFC+ males treated with IFN-γ neutralization significantly suppressed excessive defensive responses to SCs or other threats (Figures 5D–5G).

(L) Changes in GCaMP6s responses to conspecific after experiencing socially cued threat and corresponding AUC analysis during cue presentation in male SFC+ WT mice.
(M) Same as (L), but for male SFC+ Cd177-deficient mice.
(N) Comparison of changed reactivity of GCaMP6s to conspecific between Cd177-deficient mice and their littermates.
(O) Schematic of the test of GCaMP6s responses to POE in SFC+ mice before and after social exposure.
(P) Changes in GCaMP6s responses to POE after experiencing socially cued threat and corresponding AUC analysis during odor presentation in male SFC+ WT mice.
(Q) Same as (P), but for male SFC+ Cd177-deficient mice.
(R) Same as (N), but for POE. Dots represent individual mice. ns $p > 0.05$, $^*p < 0.05$, $^{**}p < 0.01$.
See also Figure S3.

Please cite this article in press as: Wu et al., Meningeal neutrophil immune signaling influences behavioral adaptation following threat, Neuron (2024), https://doi.org/10.1016/j.neuron.2024.10.018

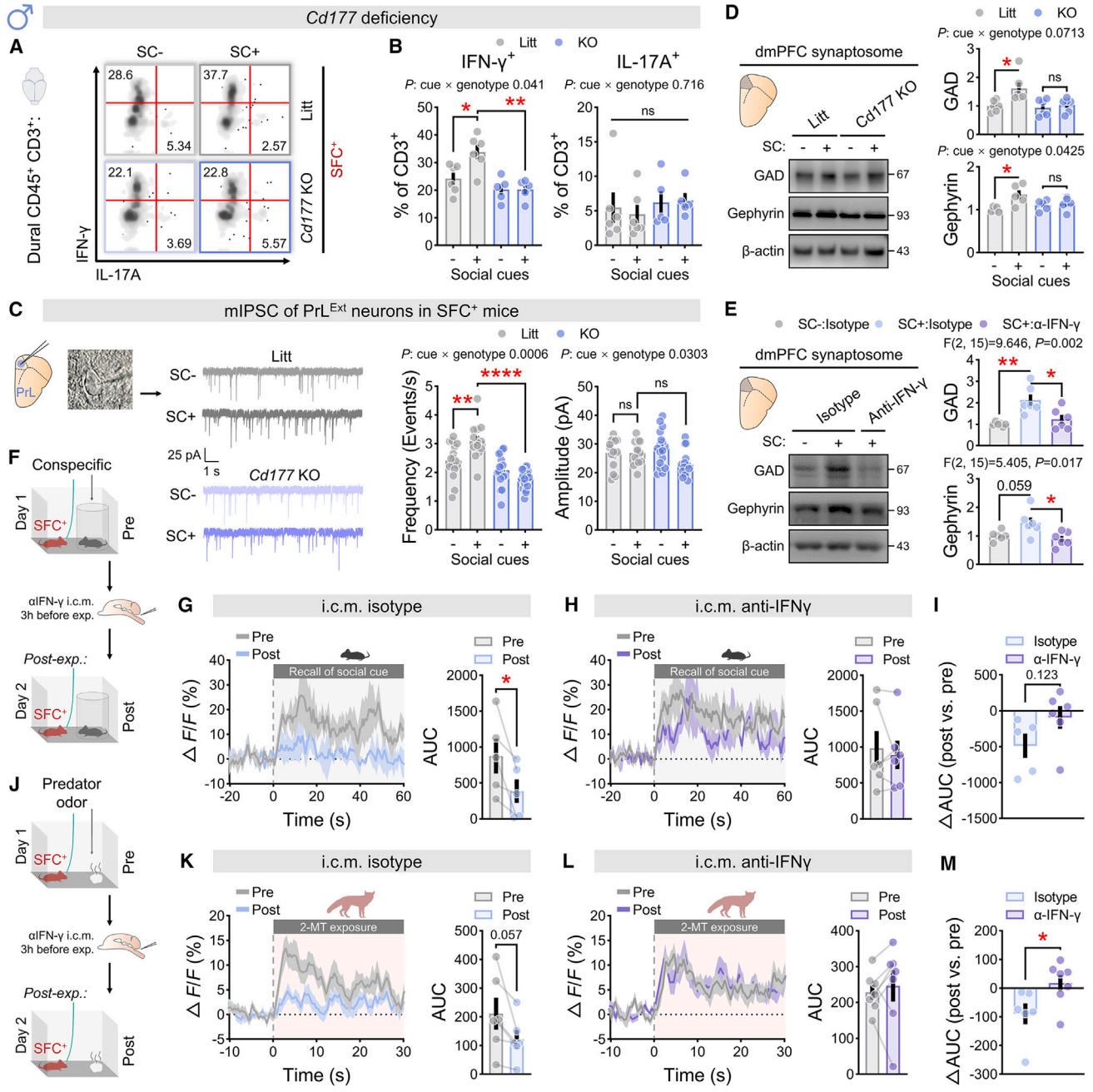

Figure 4. CD177 orchestrates IFN-γ-mediated prefrontal inhibition

(A and B) Representative density plots (A) and quantification (B) of IFN-γ$^+$ and IL-17A$^+$ T cell frequency in the dura mater from male SFC+ Cd177-deficient mice and their littermates 1 h after exposure to SCs or absence thereof, gated on CD45$^+$ CD3$^+$ cells.

(C) Representative mIPSC traces, as well as quantification of average frequency and amplitude recorded from layer 2/3 PrL pyramidal neurons of brain slices collected from SFC+ mice 1 h after exposure to SCs or absence thereof (neurons from 4 mice per group).

(D) Western blot analysis of GAD and gephyrin in the synaptosome fraction of dmPFC collected from SFC+ mice 1 h after exposure to SCs or absence thereof (n = 5–6 independent samples per group).

(E) Effects of intracisternal injection of αIFN-γ neutralizing antibodies on the expression of GAD and gephyrin in the synaptosome fraction of dmPFC (n = 6 independent samples per group).

(F) Schematic of the test of GCaMP6s responses to conspecific after αIFN-γ pre-treatment.

(G) Changes in GCaMP6s responses to conspecific after experiencing socially cued threat and corresponding AUC analysis during cue presentation in male SFC+ WT mice treated with isotype controls.

(H) Same as (G), but for male SFC+ WT mice treated with αIFN-γ neutralizing antibodies.

(legend continued on next page)

Please cite this article in press as: Wu et al., Meningeal neutrophil immune signaling influences behavioral adaptation following threat, Neuron (2024), https://doi.org/10.1016/j.neuron.2024.10.018

We next investigated whether IFN-γ administration or concurrently inhibiting PrL^{Gad1} neurons affects post-exposure defensive reactivity in Cd177-deficient mice. We first transduced hM4D(Gi) into PrL^{Gad1} neurons by injecting inhibitory DREADD AAVs under the control of Gad1 promoter into the PrL of Cd177-deficient mice (Figures 5H and 5I). A single injection of recombinant IFN-γ into the CSF of male SFC+ Cd177-deficient mice 1 h before post-test reduced the expression of defensive behaviors evoked by SCs (Figure 5K), EPM (Figures 5M and S5D), and POE (Figure 5N). Chemogenetically inhibiting PrL^{Gad1} neurons blocked these effects of IFN-γ administration (Figures 5K–5N). IFN-γ reportedly primes microglia, which can also elevate GABAergic tone.[46,47] Microglial activation markers remained unchanged after SC exposure or IFN-γ treatment (Figures S5E–S5G), suggesting a GABAergic neuronal effect that may be independent of microglial priming. These results indicate the meningeal CD177-IFN-γ signaling axis mediates behavioral effects, likely by fostering the control of emotional episodes by strengthening prelimbic neural inhibition.

Meningeal immune signaling amenable to context-specific sex hormonal modulation

Our experiments revealed a potential typological dependence of cues and sex differences in MN responses to cued threats, suggesting a sexually dimorphic factor controlling meningeal immune signaling. Testosterone, a "social hormone"[48] that exhibits pulsatile secretion in response to social stimuli in males.[49] Exposure to SCs increased circulating testosterone in male SFC+ mice but not in females or acoustic exposure (Figures S6A and S6B). To assess the effects of socially relevant testosterone response on MN CD177, we tested three additional stimulus models (Figure 6A). Male mice showed increased circulating testosterone in response to same-sex intruders and potential mates but not to acute restraint stress (Figure 6A). Notably, only social intruder stimuli significantly upregulated MN CD177 levels (Figure 6B). Both social intrusions and social threat cueing contain intrinsic or conditioned warning values. We intuited that testosterone's effect on MNs may be contingent upon the internal state of individuals, wherein threatened homeostasis potentially fosters or magnifies this effect.

To test the combined effect of testosterone and stress on MNs, we administered exogenous testosterone to male mice in a natural state or under restraint stress (Figure 6C). While a single testosterone injection minimally altered CD177 MFI on MNs, concurrent testosterone treatment with restraint stress significantly upregulated it (Figure 6D). These data support the idea that testosterone as a regulator of neutrophils amplifies MN priming, aligning with the reported positive role of androgen signaling in the number, maturation, or function of neutrophils.[50–52]

The context-dependent regulation by testosterone raises the possibility that transient threat experience may shape a stressful internal milieu. Acute stress-responsive peptides can independently prime neutrophils and modulate their function,[53–56] then one would predict that socially driven testosterone responses in males may further promote neutrophil state transitions on this basis. To preliminarily test this prediction, we focused on endothelin-1 (ET-1), a conserved stress-responsive molecule[57–59] that can independently prime neutrophils.[56] We found that stimulation of murine neutrophils with low concentrations of ET-1 or testosterone did not significantly affect cell surface CD177 levels; however, when testosterone was added to the medium containing ET-1, the MFI of CD177 was induced (Figures 6E and 6F). Androgen signaling reportedly promotes STAT3 disinhibition and ERK activation in neutrophils,[50] which may be a molecular basis for fueling priming.

In support of a role for testosterone reactivity in orchestrating meningeal immunity and behavioral response, castration of SFC+ male mice reduced CD177 levels on MNs and the frequency of IFN-γ-producing meningeal CD3$^+$ T cells after exposure to SCs (Figures 6G and S6C). These mice maintained the SC-evoked avoidance responses, unlike sham-operated mice (Figure 6H). A single post-exposure testosterone treatment restored CD177 levels (Figure S6D), CD3$^+$ IFN-γ$^+$ T cell frequency (Figure 6G), and inhibitory social avoidance (Figure 6H). Long-term testosterone replacement did not affect behavioral responses (Figure S6C), suggesting gonadal feedback to SCs, rather than homeostatic testosterone, may transmit regulatory signals.

To further confirm the foregoing findings, we repeated the post-exposure single testosterone treatment in female SFC+ mice. Females treated with a single testosterone exhibited significantly upregulated CD177 levels on MNs (Figure S6E), meningeal frequency of IFN-γ$^+$ CD3$^+$ T cells (Figure S6F), and reduced social avoidance response (Figure S6G). Critically, these effects were blocked in Cd177-deficient SFC+ females (Figures S6F and S6G).

Whether these observations can be generalized to responses to threat-predicting non-SCs, where the presence of environmental social signals unrelated to the threat itself may also impact meningeal immune homeostasis and the behavioral regulation it executes. To this end, mice were exposed to acoustically cued threats paired with opposite-sex conspecifics (Figure 6I). Social pairing induced upregulation of circulating testosterone levels in male mice exposed to acoustic cues (Figure 6J). Furthermore, male-biased upregulation of CD177 on MNs (Figure 6K), the frequency of meningeal CD3$^+$ IFN-γ$^+$ T cells (Figure 6L), and short-term adaptation to sound-evoked fear (Figures 6M–6O) were also observed. Taken together, our results propose that separable perceptions of SCs and threat values convergently drive meningeal immune activity, a process that is highly regulated by androgen responsiveness.

(I) Comparison of changed reactivity of GCaMP6s to conspecific between male SFC+ WT mice treated with αIFN-γ neutralizing antibodies and isotype controls.
(J) Schematic of the test of GCaMP6s responses to POE after αIFN-γ pre-treatment.
(K) Changes in GCaMP6s responses to POE after experiencing socially cued threat and corresponding AUC analysis during odor presentation in male SFC+ WT mice treated with isotype controls.
(L) Same as (K), but for male SFC+ WT mice treated with αIFN-γ neutralizing antibodies.
(M) Same as (I), but for POE. Dots represent neurons (C) or individual mice. ns $p > 0.05$, *$p < 0.05$, **$p < 0.01$, ****$p < 0.0001$.
See also Figure S4.

Please cite this article in press as: Wu et al., Meningeal neutrophil immune signaling influences behavioral adaptation following threat, Neuron (2024), https://doi.org/10.1016/j.neuron.2024.10.018

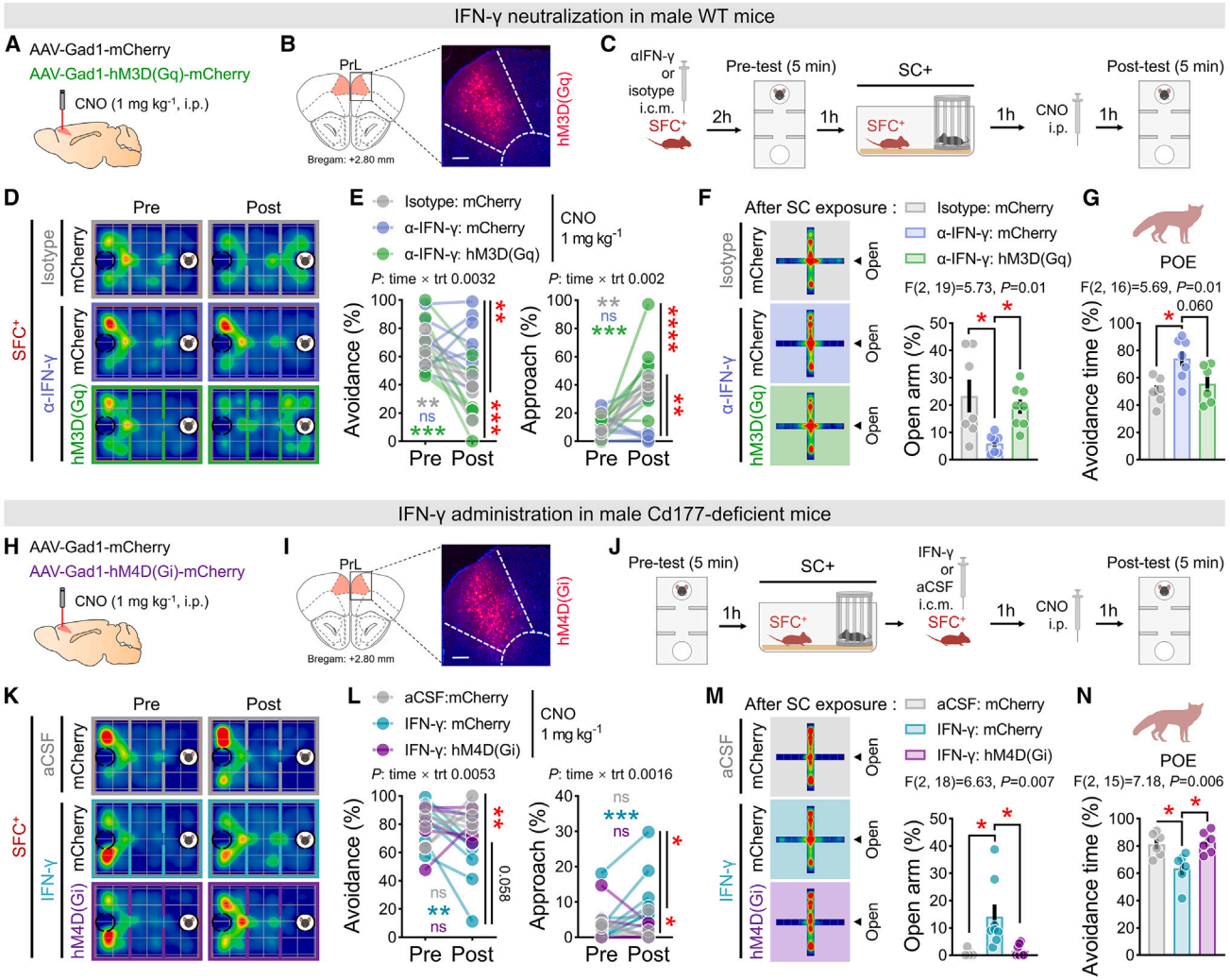

Figure 5. IFN-γ-driven suppression of threat-motivated behavior requires PrL^{Gad1} neurons

(A and B) Schematic (A) and representative image (B) of AAV-dependent expression of excitatory DREADD hM3D(Gq) in the PrL. Scale bar, 250 μm.

(C) Experimental schema for IFN-γ neutralization in male WT mice.

(D) Average heatmaps showing location and time during SATs before and after exposure to SCs in male SFC+ WT mice treated with isotype controls, αIFN-γ or αIFN-γ combined with chemogenetic activation of PrL^{Gad1} neurons.

(E) Changes in the relative time spent on social avoidance and approach after exposure to SCs.

(F and G) EPM- (F) and POE-evoked (G) avoidance behaviors after exposure to SCs in male SFC+ WT mice treated with isotype controls, αIFN-γ or αIFN-γ combined with chemogenetic activation of PrL^{Gad1} neurons.

(H and I) Schematic (H) and representative image (I) of AAV-dependent expression of inhibitory DREADD hM4D(Gi) in the PrL. Scale bar, 250 μm.

(J) Experimental schema for IFN-γ administration in male Cd177-deficient mice.

(K) Average heatmaps showing location and time during SATs before and after exposure to SCs in male SFC+ Cd177-deficient mice treated with aCSF, IFN-γ, or IFN-γ combined with chemogenetic inhibition of PrL^{Gad1} neurons.

(L) Changes in the relative time spent on social avoidance and approach after exposure to SCs.

(M and N) EPM- (M) and POE-evoked (N) avoidance behaviors after exposure to SCs in male SFC+ Cd177-deficient mice treated with aCSF, IFN-γ, or IFN-γ combined with chemogenetic inhibition of PrL^{Gad1} neurons. Dots represent individual mice. ns $p > 0.05$, *$p < 0.05$, **$p < 0.01$, ***$p < 0.001$, ****$p < 0.0001$. See also Figure S5.

Sex-specific neutrophil priming signatures in human threat responses

Anxious or traumatic individuals often attend to and over-evaluate facial cues due to altered sensory gating.[60–63] Environmental social information may be inadvertently processed alongside primary non-social danger signals. Moreover, human males appear to be sensitive to emotional cues in faces and exhibit greater psychophysiological activation,[64,65] including elevated testosterone response.[66] Thus, the sex-specific hormone-neutrophil-emotion regulatory axis may extend to human responses to general threats.

Please cite this article in press as: Wu et al., Meningeal neutrophil immune signaling influences behavioral adaptation following threat, Neuron (2024), https://doi.org/10.1016/j.neuron.2024.10.018

CellPress

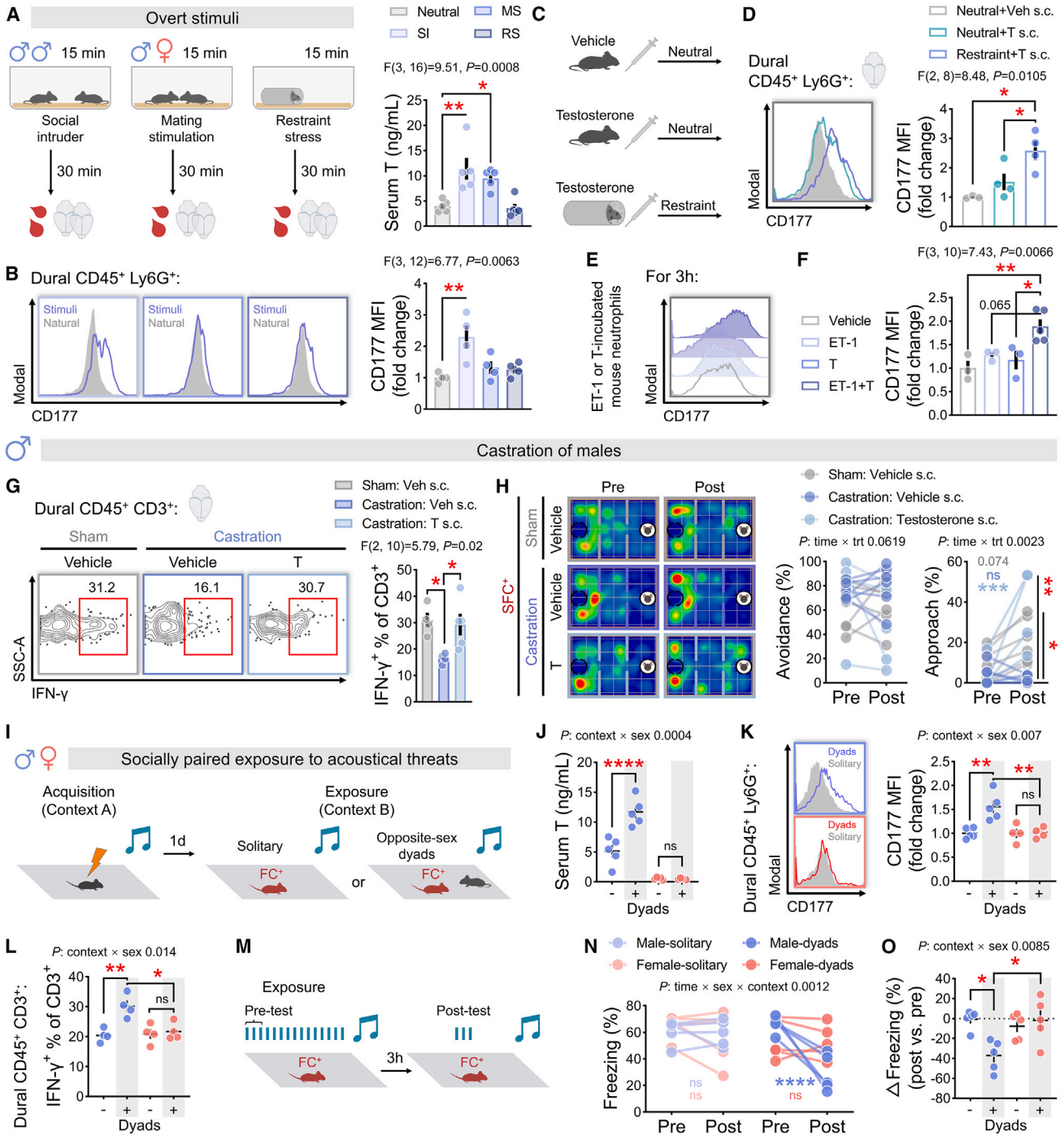

Figure 6. Meningeal immune signaling amenable to context-specific sex hormonal modulation

(A) Schematic of the social or non-social stimuli and the circulating testosterone levels measured by ELISA.

(B) Representative histograms of CD177 levels on MNs and quantification of the relative MFI changes of CD177 induced by social or non-social stimuli, gated on CD45$^+$ Ly6G$^+$ cells.

(C and D) Schematic of restraint stress combined with testosterone injection (C) and quantification (D) of the relative MFI changes of CD177, gated on CD45$^+$ Ly6G$^+$ cells.

(E and F) Representative histograms (E) of CD177 levels on MNs and quantification (F) of the relative MFI changes of CD177 induced by *in vitro* incubation of ET-1, testosterone, or ET-1 combined with testosterone.

(G) Representative contour plots and quantification of meningeal IFN-γ$^+$ T cell frequency in castrated or sham-operated male SFC+ WT mice 1 h after exposure to SCs, gated on CD45$^+$ CD3$^+$ cells.

(legend continued on next page)

Please cite this article in press as: Wu et al., Meningeal neutrophil immune signaling influences behavioral adaptation following threat, Neuron (2024), https://doi.org/10.1016/j.neuron.2024.10.018

Re-analysis of published datasets allowed us to evaluate aforementioned possibility. Human blood gene expression data came from patients with anxiety disorders undergoing fear exposure under the guidance of therapists.[67,68] CIBERSORT estimation[69] showed only neutrophil numbers significantly increased post-exposure, returning to baseline after 24 h (Figures S7A and S7B). This reversible increase in the number of circulating neutrophils may be part of an acute stress response.[9] Microarray studies indicated neutrophil priming accompanies transcriptional changes,[70,71] and we next sought to identify these gene signatures to characterize neutrophil states. Additionally, we generated signature gene sets for androgen and stress hormone-induced transcriptional activation to assess individual testosterone reactivity and stress levels (Figures 7A–7E), as detailed in the STAR Methods.

Gene set variation analysis (GSVA) revealed a sexually dimorphic blood transcriptional response after exposure. Males but not females showed fluctuations in neutrophil priming signatures (NPSs) and significant NPS enrichment post-exposure (Figure 7F). Male-biased exposure-induced enrichment was also found in the canonical pathway of neutrophil degranulation (Figure S7B). Correspondingly, androgen-induced gene signatures in the male blood increased significantly in response to exposure compared with females (Figure 7G), suggesting sex-specific testosterone responses during human threat anticipation.

Cortisol release, a stress-sensitive biological mechanism, is triggered during threat anticipation and exposure and decayed after the end of exposure.[72,73] We were interested in changes in blood cortisol-induced gene signatures within 24 h post-exposure, which may reflect the persistence or resolution of emotional states after exposure. Male blood transcripts showed more and consistent negative enrichment 24 h after exposure compared with females (Figure 7H). Interestingly, the magnitude of the exposure-induced shifts in NPS was more correlated with shifts in stress-related gene signatures in males than females (Figure 7I). These results suggest a parallel relationship among testosterone signaling, neutrophil activity, and emotional state in the human threat response (Figure 7J).

DISCUSSION

The immune system is controlled by and influences emotional states, but the precise mechanisms remain unclear. Here, we propose a model where dura-resident neutrophils sense conspecific cues that transmit danger signals and are primed in a sex-dependent manner. These neutrophils drive meningeal Th1-like immunity via CD177, negatively modulating the defensive response through IFN-γ-mediated prefrontal inhibition. Our findings position meningeal immunity at the intersection of psychosocial challenges and behavior, suggesting neutrophils as accessible targets for emotional regulation.

The primed phenotype of MNs was likely triggered synergistically by androgen signaling and stress-responsive peptides into the circulation, stemming from the perception of external stimuli. Such factors have been shown to positively regulate neutrophil function.[50–56] Collaboratively, the communication among these threat-responsive elements at the peripheral-meningeal-brain interface rapidly reshaped male emotional states, fostering adaptation to threat. Approaching dangerous conspecifics is risky, risking injury and pathogen exposure. Priming immune defenses may mitigate infection risk when approaching, reflecting an immune-mediated sociability-infection trade-off. Evolutionarily, this mechanism may advantage males in frequent social challenges by enhancing immunity and encouraging approach.

The human dmPFC processes complex social information[74] and assesses threatening situations in response to conditioned stimuli,[75] acting as a source of negative affect. These functional insights support the role of this brain region as a key site for perceiving social stimuli and interpreting threats. The mouse PrL region is anatomically and functionally coupled to the human dmPFC, and it appears that they are highly close to the immunologically active dural sinuses.[42,76] Chemogenetic inhibition of PrL^{Gad1} neurons blocked behavioral effects of CSF-delivered IFN-γ, linking this cortical region to meningeal immunity. Remarkably, L1 of the PrL is located in a dominant position for this CSF-contacting construct,[39] which is mainly composed of GABAergic neuronal cell somas and has been reported to strongly inhibit L2/3 excitatory neurons.[77] These observations actually reinforce the notion that meningeal-driven immune signaling preferentially tunes cortical inhibition.

Excitatory inputs from the PrL to basolateral amygdala (BLA) are associated with social withdrawal and fear expression.[78] While the BLA, an internal nucleus, may have limited direct response to CSF-derived signals,[35] a direct regulatory role of blood testosterone can't be ruled out. Testosterone administration promotes threat approach and social dominance, increasing amygdala responses,[79] while reducing amygdala-prefrontal connectivity and shifting to subcortical regions.[80] Thus, modification of the larger emotional circuits involving the PFC and amygdala is likely a major aspect of the sophisticated role of testosterone. Our data highlight a more indirect scenario: testosterone facilitates PrL inhibition by a meningeal immune axis, potentially regulating threat responses top-down.

(H) Left: average heatmaps showing location and time during SATs before and after exposure to SCs in castrated or sham-operated male SFC+ WT mice treated with vehicle or testosterone; right: changes in the relative time spent on social avoidance and approach after exposure to SCs.
(I) Schematic of the socially paired exposure to acoustical threats.
(J) Changes in circulating testosterone levels in male and female mice exposed to conditioned acoustic stimuli alone or in pairs.
(K) Same as (J), but for CD177 levels on MNs, gated on $CD45^+$ $Ly6G^+$ cells.
(L) Same as (J), but for meningeal IFN-γ^+ T cell frequency, gated on $CD45^+$ $CD3^+$ cells.
(M) Schematic of the test of acoustically evoked defensive response after exposure.
(N) Changes in cue-evoked freezing of male and female mice before and after exposed to conditioned acoustic stimuli alone or in pairs.
(O) Comparison of changed defensive responses to acoustical cues. T, testosterone. Dots represent independent experiments (F) or individual mice. ns $p > 0.05$, $^*p < 0.05$, $^{**}p < 0.01$, $^{***}p < 0.001$, $^{****}p < 0.0001$.
See also Figure S6.

Please cite this article in press as: Wu et al., Meningeal neutrophil immune signaling influences behavioral adaptation following threat, Neuron (2024), https://doi.org/10.1016/j.neuron.2024.10.018

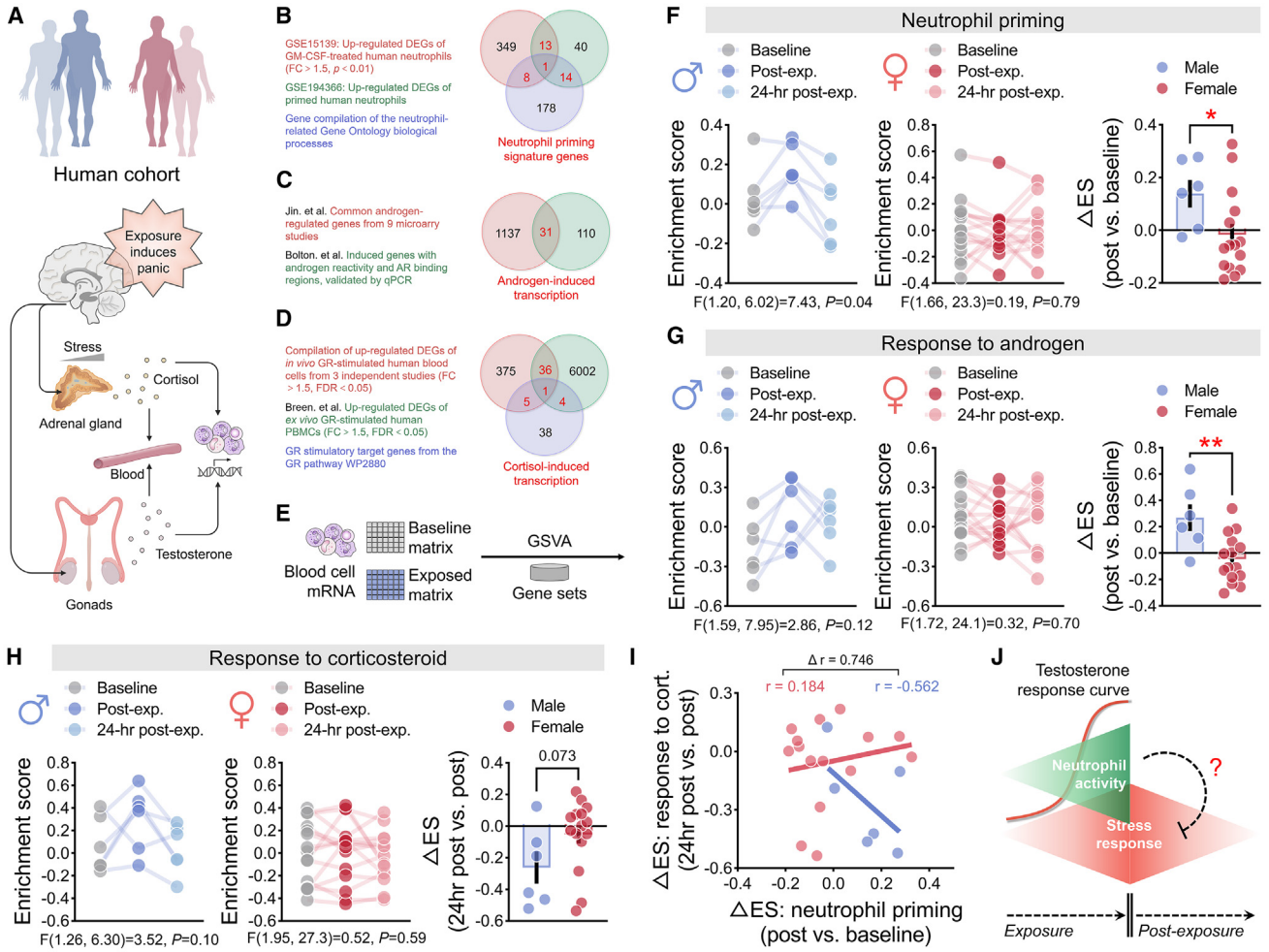

Figure 7. Sex-specific neutrophil priming signatures in human threat responses

(A) Characterization of neutrophil, testosterone, and stress hormone responses after fear exposure in human subjects using blood cell transcriptome.

(B–D) Venn diagram showing signatures of neutrophil priming and androgen- and cortisol-induced transcriptional activation.

(E) Schematic of the GSVA.

(F) Left and middle: trajectories of post-exposure NPS in men and women; right: comparison of the magnitude of changes between men and women.

(G) Same as (J), but for androgen-induced gene signatures.

(H) Same as (J), but for cortisol-induced gene signatures.

(I) Correlation analysis between the changes of NPS induced by exposure and the changes of cortisol-induced gene signatures within 24 h of the end of exposure.

(J) Proposed model for the dynamics of sex hormone, neutrophil activity, and stress response in males exposed to fear-provoking cues. Blue symbols, men; pink symbols, women. Dots represent individual subjects. *$p < 0.05$, **$p < 0.01$.

See also Figure S7.

Hormonal fluctuations triggered by reproductive events may contribute to sex differences in anxiety. Changes during menstruation and reproduction can increase anxiety in women.[81,82] While much focus has been placed on female emotional vulnerability, male resistance mechanisms are less explored. We propose that rapid testosterone response to SCs reduces negative emotions and avoidance in male mice through immune signals at the meningeal interface, aligning with findings that testosterone promotes social approach in men.[83] SCs may trigger immune responses in an unexpectedly sensitive manner, as merely viewing photographs containing negative SCs has been reported to enhance the induction of pro-inflammatory cytokines in blood leukocytes.[84] We found that IFN-γ acts like a neuromodulator, which regulates neural and behavioral threat reactivity. Interestingly, IFN-γ is one of the few pro-inflammatory cytokines that is reduced in anxiety disorders.[85] Overall, a comprehensive, sometimes personalized, endocrine-immune-neural circuit may shape behavioral traits and resilience following stress events.

In summary, our findings support the notion that immune cell populations inhabiting at brain boundaries possess "wireless" capabilities to access neuronal circuits, supporting brain homeostasis.[86] Neutrophils, within the dura mater, represent regulators of neural processes, broadening their function from

orchestrating immune defenses to influencing neuro-based defensive reactions. Ultimately, these intricate mechanisms are dedicated to maintaining host homeostasis in the face of complex physical and social environmental challenges.

RESOURCE AVAILABILITY

Lead contact

Further information and requests for resources and reagents should be directed to and will be fulfilled by the lead contact, Zhifang Dong (zfdong@cqmu.edu.cn).

Materials availability

This study did not generate new or unique reagents.

Data and code availability

All data reported in this paper will be shared by the lead contact upon request. This paper does not report original code.

ACKNOWLEDGMENTS

This work was supported by the National Natural Science Foundation of China (32371030, 82071395, 32170766, and 82100087), the Natural Science Foundation of Chongqing (CSTB2024NSCQ-LZX0008), and the CQMU Program for Youth Innovation in Future Medicine (W0044). We thank BioRender for help creating parts of the schematic figures.

AUTHOR CONTRIBUTIONS

B.W. and L.M. conceived the study, performed experiments, and wrote the manuscript. Y.Z., J.L., Q.T., and Y.P. assisted with experimental procedures. J.L. performed *ex vivo* electrophysiology and analysis. C.R. and Z.D. contributed essential reagents or tools and critically reviewed the manuscript. Z.D. supervised all the experiments and the writing of the manuscript. All authors commented on it.

DECLARATION OF INTERESTS

The authors declare no competing interests.

STAR★METHODS

Detailed methods are provided in the online version of this paper and include the following:

SUPPLEMENTAL INFORMATION

Supplemental information can be found online at https://doi.org/10.1016/j.neuron.2024.10.018.

Received: August 7, 2023
Revised: May 27, 2024
Accepted: October 17, 2024
Published: November 18, 2024

REFERENCES

1. Cannon, W. (1932). The Wisdom of the Body (WW Norton & Company. Inc.).
2. LeDoux, J., and Daw, N.D. (2018). Surviving threats: neural circuit and computational implications of a new taxonomy of defensive behaviour. Nat. Rev. Neurosci. *19*, 269–282. https://doi.org/10.1038/nrn.2018.22.
3. Malezieux, M., Klein, A.S., and Gogolla, N. (2023). Neural Circuits for Emotion. Annu. Rev. Neurosci. *46*, 211–231. https://doi.org/10.1146/annurev-neuro-111020-103314.
4. Neuberg, S.L., Kenrick, D.T., and Schaller, M. (2011). Human threat management systems: self-protection and disease avoidance. Neurosci. Biobehav. Rev. *35*, 1042–1051. https://doi.org/10.1016/j.neubiorev.2010.08.011.
5. Bishop, S.J. (2007). Neurocognitive mechanisms of anxiety: an integrative account. Trends Cogn. Sci. *11*, 307–316. https://doi.org/10.1016/j.tics.2007.05.008.
6. McEwen, B.S. (2007). Physiology and neurobiology of stress and adaptation: central role of the brain. Physiol. Rev. *87*, 873–904. https://doi.org/10.1152/physrev.00041.2006.
7. Westlin, C., Theriault, J.E., Katsumi, Y., Nieto-Castanon, A., Kucyi, A., Ruf, S.F., Brown, S.M., Pavel, M., Erdogmus, D., Brooks, D.H., et al. (2023). Improving the study of brain-behavior relationships by revisiting basic assumptions. Trends Cogn. Sci. *27*, 246–257. https://doi.org/10.1016/j.tics.2022.12.015.
8. Medzhitov, R., and Iwasaki, A. (2024). Exploring new perspectives in immunology. Cell *187*, 2079–2094. https://doi.org/10.1016/j.cell.2024.03.038.
9. Davis, A.K., Maney, D.L.M.C., and Maerz, J.C. (2008). The use of leukocyte profiles to measure stress in vertebrates: a review for ecologists. Funct. Ecol. *22*, 760–772. https://doi.org/10.1111/j.1365-2435.2008.01467.x.
10. Poller, W.C., Downey, J., Mooslechner, A.A., Khan, N., Li, L., Chan, C.T., McAlpine, C.S., Xu, C., Kahles, F., He, S., et al. (2022). Brain motor and fear circuits regulate leukocytes during acute stress. Nature *607*, 578–584. https://doi.org/10.1038/s41586-022-04890-z.
11. Summers, C., Rankin, S.M., Condliffe, A.M., Singh, N., Peters, A.M., and Chilvers, E.R. (2010). Neutrophil kinetics in health and disease. Trends Immunol. *31*, 318–324. https://doi.org/10.1016/j.it.2010.05.006.

12. Burn, G.L., Foti, A., Marsman, G., Patel, D.F., and Zychlinsky, A. (2021). The Neutrophil. Immunity *54*, 1377–1391. https://doi.org/10.1016/j.immuni.2021.06.006.

13. Nicolás-Ávila, J.Á., Adrover, J.M., and Hidalgo, A. (2017). Neutrophils in Homeostasis, Immunity, and Cancer. Immunity *46*, 15–28. https://doi.org/10.1016/j.immuni.2016.12.012.

14. Mantovani, A., Cassatella, M.A., Costantini, C., and Jaillon, S. (2011). Neutrophils in the activation and regulation of innate and adaptive immunity. Nat. Rev. Immunol. *11*, 519–531. https://doi.org/10.1038/nri3024.

15. Alves de Lima, K., Rustenhoven, J., and Kipnis, J. (2020). Meningeal Immunity and Its Function in Maintenance of the Central Nervous System in Health and Disease. Annu. Rev. Immunol. *38*, 597–620. https://doi.org/10.1146/annurev-immunol-102319-103410.

16. Van Hove, H., Martens, L., Scheyltjens, I., De Vlaminck, K., Pombo Antunes, A.R., De Prijck, S., Vandamme, N., De Schepper, S., Van Isterdael, G., Scott, C.L., et al. (2019). A single-cell atlas of mouse brain macrophages reveals unique transcriptional identities shaped by ontogeny and tissue environment. Nat. Neurosci. *22*, 1021–1035. https://doi.org/10.1038/s41593-019-0393-4.

17. Niu, C., Yu, J., Zou, T., Lu, Y., Deng, L., Yun, H., Si, C.Y., Wu, X., Jiang, H., Guo, T., et al. (2022). Identification of hematopoietic stem cells residing in the meninges of adult mice at steady state. Cell Rep. *41*, 111592. https://doi.org/10.1016/j.celrep.2022.111592.

18. Kolabas, Z.I., Kuemmerle, L.B., Perneczky, R., Förstera, B., Ulukaya, S., Ali, M., Kapoor, S., Bartos, L.M., Büttner, M., Caliskan, O.S., et al. (2023). Distinct molecular profiles of skull bone marrow in health and neurological disorders. Cell *186*, 3706–3725.e29. https://doi.org/10.1016/j.cell.2023.07.009.

19. Chen, P., and Hong, W. (2018). Neural Circuit Mechanisms of Social Behavior. Neuron *98*, 16–30. https://doi.org/10.1016/j.neuron.2018.02.026.

20. Eisenberger, N.I., Moieni, M., Inagaki, T.K., Muscatell, K.A., and Irwin, M.R. (2017). In Sickness and in Health: The Co-Regulation of Inflammation and Social Behavior. Neuropsychopharmacology *42*, 242–253. https://doi.org/10.1038/npp.2016.141.

21. Sengeløv, H., Kjeldsen, L., and Borregaard, N. (1993). Control of exocytosis in early neutrophil activation. J. Immunol. *150*, 1535–1543. https://doi.org/10.4049/jimmunol.150.4.1535.

22. Lacy, P. (2006). Mechanisms of degranulation in neutrophils. Allergy Asthma Clin. Immunol. *2*, 98–108. https://doi.org/10.1186/1710-1492-2-3-98.

23. Miralda, I., Uriarte, S.M., and McLeish, K.R. (2017). Multiple Phenotypic Changes Define Neutrophil Priming. Front. Cell. Infect. Microbiol. *7*, 217. https://doi.org/10.3389/fcimb.2017.00217.

24. Dunsmoor, J.E., Niv, Y., Daw, N., and Phelps, E.A. (2015). Rethinking Extinction. Neuron *88*, 47–63. https://doi.org/10.1016/j.neuron.2015.09.028.

25. Evans, D.A., Stempel, A.V., Vale, R., and Branco, T. (2019). Cognitive Control of Escape Behaviour. Trends Cogn. Sci. *23*, 334–348. https://doi.org/10.1016/j.tics.2019.01.012.

26. Baker, K.D., McNally, G.P., and Richardson, R. (2013). Memory retrieval before or after extinction reduces recovery of fear in adolescent rats. Learn. Mem. *20*, 467–473. https://doi.org/10.1101/lm.031989.113.

27. Corey, S.J., and Rosoff, P.M. (1989). Granulocyte-macrophage colony-stimulating factor primes neutrophils by activating a pertussis toxin-sensitive G protein not associated with phosphatidylinositol turnover. J. Biol. Chem. *264*, 14165–14171. https://doi.org/10.1016/S0021-9258(18)71657-8.

28. Ramadass, M., Johnson, J.L., and Catz, S.D. (2017). Rab27a regulates GM-CSF-dependent priming of neutrophil exocytosis. J. Leukoc. Biol. *101*, 693–702. https://doi.org/10.1189/jlb.3AB0416-189RR.

29. Uriarte, S.M., Powell, D.W., Luerman, G.C., Merchant, M.L., Cummins, T.D., Jog, N.R., Ward, R.A., and McLeish, K.R. (2008). Comparison of proteins expressed on secretory vesicle membranes and plasma membranes of human neutrophils. J. Immunol. *180*, 5575–5581. https://doi.org/10.4049/jimmunol.180.8.5575.

30. Stroncek, D.F. (2007). Neutrophil-specific antigen HNA-2a, NB1 glycoprotein, and CD177. Curr. Opin. Hematol. *14*, 688–693. https://doi.org/10.1097/MOH.0b013e3282efed9e.

31. Kaiser, R., Gold, C., Joppich, M., Loew, Q., Akhalkatsi, A., Mueller, T.T., Offensperger, F., Droste Zu Senden, A., Popp, O., di Fina, L., et al. (2024). Peripheral priming induces plastic transcriptomic and proteomic responses in circulating neutrophils required for pathogen containment. Sci. Adv. *10*, eadl1710. https://doi.org/10.1126/sciadv.adl1710.

32. Xie, Q., Klesney-Tait, J., Keck, K., Parlet, C., Borcherding, N., Kolb, R., Li, W., Tygrett, L., Waldschmidt, T., Olivier, A., et al. (2015). Characterization of a novel mouse model with genetic deletion of CD177. Protein Cell *6*, 117–126. https://doi.org/10.1007/s13238-014-0109-1.

33. Cugurra, A., Mamuladze, T., Rustenhoven, J., Dykstra, T., Beroshvili, G., Greenberg, Z.J., Baker, W., Papadopoulos, Z., Drieu, A., Blackburn, S., et al. (2021). Skull and vertebral bone marrow are myeloid cell reservoirs for the meninges and CNS parenchyma. Science *373*, eabf7844. https://doi.org/10.1126/science.abf7844.

34. Brioschi, S., Wang, W.L., Peng, V., Wang, M., Shchukina, I., Greenberg, Z.J., Bando, J.K., Jaeger, N., Czepielewski, R.S., Swain, A., et al. (2021). Heterogeneity of meningeal B cells reveals a lymphopoietic niche at the CNS borders. Science *373*, eabf9277. https://doi.org/10.1126/science.abf9277.

35. Iliff, J.J., Wang, M., Liao, Y., Plogg, B.A., Peng, W., Gundersen, G.A., Benveniste, H., Vates, G.E., Deane, R., Goldman, S.A., et al. (2012). A paravascular pathway facilitates CSF flow through the brain parenchyma and the clearance of interstitial solutes, including amyloid β. Sci. Transl. Med. *4*, 147ra111. https://doi.org/10.1126/scitranslmed.3003748.

36. Green, T.A., Baracz, S.J., Everett, N.A., Robinson, K.J., and Cornish, J.L. (2020). Differential effects of GABAA receptor activation in the prelimbic and orbitofrontal cortices on anxiety. Psychopharmacology *237*, 3237–3247. https://doi.org/10.1007/s00213-020-05606-9.

37. Sotres-Bayon, F., and Quirk, G.J. (2010). Prefrontal control of fear: more than just extinction. Curr. Opin. Neurobiol. *20*, 231–235. https://doi.org/10.1016/j.conb.2010.02.005.

38. Calhoon, G.G., and Tye, K.M. (2015). Resolving the neural circuits of anxiety. Nat. Neurosci. *18*, 1394–1404. https://doi.org/10.1038/nn.4101.

39. Filiano, A.J., Xu, Y., Tustison, N.J., Marsh, R.L., Baker, W., Smirnov, I., Overall, C.C., Gadani, S.P., Turner, S.D., Weng, Z., et al. (2016). Unexpected role of interferon-γ in regulating neuronal connectivity and social behaviour. Nature *535*, 425–429. https://doi.org/10.1038/nature18626.

40. Alves de Lima, K., Rustenhoven, J., Da Mesquita, S., Wall, M., Salvador, A.F., Smirnov, I., Martelossi Cebinelli, G., Mamuladze, T., Baker, W., Papadopoulos, Z., et al. (2020). Meningeal γδ T cells regulate anxiety-like behavior via IL-17a signaling in neurons. Nat. Immunol. *21*, 1421–1429. https://doi.org/10.1038/s41590-020-0776-4.

41. Jaeger, B.N., Donadieu, J., Cognet, C., Bernat, C., Ordoñez-Rueda, D., Barlogis, V., Mahlaoui, N., Fenis, A., Narni-Mancinelli, E., Beaupain, B., et al. (2012). Neutrophil depletion impairs natural killer cell maturation, function, and homeostasis. J. Exp. Med. *209*, 565–580. https://doi.org/10.1084/jem.20111908.

42. Rustenhoven, J., Drieu, A., Mamuladze, T., de Lima, K.A., Dykstra, T., Wall, M., Papadopoulos, Z., Kanamori, M., Salvador, A.F., Baker, W., et al. (2021). Functional characterization of the dural sinuses as a neuroimmune interface. Cell *184*, 1000–1016.e27. https://doi.org/10.1016/j.cell.2020.12.040.

43. Zipp, F., Bittner, S., and Schafer, D.P. (2023). Cytokines as emerging regulators of central nervous system synapses. Immunity *56*, 914–925. https://doi.org/10.1016/j.immuni.2023.04.011.

44. Döhne, N., Falck, A., Janach, G.M.S., Byvaltcev, E., and Strauss, U. (2022). Interferon-γ augments GABA release in the developing neocortex via nitric oxide synthase/soluble guanylate cyclase and constrains network activity. Front. Cell. Neurosci. *16*, 913299. https://doi.org/10.3389/fncel.2022.913299.

45. Flood, L., Korol, S.V., Ekselius, L., Birnir, B., and Jin, Z. (2019). Interferon-γ potentiates GABAA receptor-mediated inhibitory currents in rat hippocampal CA1 pyramidal neurons. J. Neuroimmunol. *337*, 577050. https://doi.org/10.1016/j.jneuroim.2019.577050.

46. Ta, T.T., Dikmen, H.O., Schilling, S., Chausse, B., Lewen, A., Hollnagel, J.O., and Kann, O. (2019). Priming of microglia with IFN-γ slows neuronal gamma oscillations in situ. Proc. Natl. Acad. Sci. USA *116*, 4637–4642. https://doi.org/10.1073/pnas.1813562116.

47. Jiang, J., Tang, B., Wang, L., Huo, Q., Tan, S., Misrani, A., Han, Y., Li, H., Hu, H., Wang, J., et al. (2022). Systemic LPS-induced microglial activation results in increased GABAergic tone: A mechanism of protection against neuroinflammation in the medial prefrontal cortex in mice. Brain Behav. Immun. *99*, 53–69. https://doi.org/10.1016/j.bbi.2021.09.017.

48. Eisenegger, C., Haushofer, J., and Fehr, E. (2011). The role of testosterone in social interaction. Trends Cogn. Sci. *15*, 263–271. https://doi.org/10.1016/j.tics.2011.04.008.

49. Zilioli, S., and Bird, B.M. (2017). Functional significance of men's testosterone reactivity to social stimuli. Front. Neuroendocrinol. *47*, 1–18. https://doi.org/10.1016/j.yfrne.2017.06.002.

50. Chuang, K.H., Altuwaijri, S., Li, G., Lai, J.J., Chu, C.Y., Lai, K.P., Lin, H.Y., Hsu, J.W., Keng, P., Wu, M.C., et al. (2009). Neutropenia with impaired host defense against microbial infection in mice lacking androgen receptor. J. Exp. Med. *206*, 1181–1199. https://doi.org/10.1084/jem.20082521.

51. Li, F., Xing, X., Jin, Q., Wang, X.M., Dai, P., Han, M., Shi, H., Zhang, Z., Shao, X., Peng, Y., et al. (2024). Sex differences orchestrated by androgens at single-cell resolution. Nature *629*, 193–200. https://doi.org/10.1038/s41586-024-07291-6.

52. Deitch, E.A., Ananthakrishnan, P., Cohen, D.B., Xu, D.Z., Feketeova, E., and Hauser, C.J. (2006). Neutrophil activation is modulated by sex hormones after trauma-hemorrhagic shock and burn injuries. Am. J. Physiol. Heart Circ. Physiol. *291*, H1456–H1465. https://doi.org/10.1152/ajpheart.00694.2005.

53. Bedoui, S., Kromer, A., Gebhardt, T., Jacobs, R., Raber, K., Dimitrijevic, M., Heine, J., and von Hörsten, S. (2008). Neuropeptide Y receptor-specifically modulates human neutrophil function. J. Neuroimmunol. *195*, 88–95. https://doi.org/10.1016/j.jneuroim.2008.01.012.

54. Sharp, B.M., Keane, W.F., Suh, H.J., Gekker, G., Tsukayama, D., and Peterson, P.K. (1985). Opioid peptides rapidly stimulate superoxide production by human polymorphonuclear leukocytes and macrophages. Endocrinology *117*, 793–795. https://doi.org/10.1210/endo-117-2-793.

55. Czepielewski, R.S., Porto, B.N., Rizzo, L.B., Roesler, R., Abujamra, A.L., Pinto, L.G., Schwartsmann, G., Cunha, F.Q., and Bonorino, C. (2012). Gastrin-releasing peptide receptor (GRPR) mediates chemotaxis in neutrophils. Proc. Natl. Acad. Sci. USA *109*, 547–552. https://doi.org/10.1073/pnas.1110996109.

56. Hafström, I., Ringertz, B., Lundeberg, T., and Palmblad, J. (1993). The effect of endothelin, neuropeptide Y, calcitonin gene-related peptide and substance P on neutrophil functions. Acta Physiol. Scand. *148*, 341–346. https://doi.org/10.1111/j.1748-1716.1993.tb09565.x.

57. Treiber, F.A., Kapuku, G.K., Davis, H., Pollock, J.S., and Pollock, D.M. (2002). Plasma endothelin-1 release during acute stress: role of ethnicity and sex. Psychosom. Med. *64*, 707–713. https://doi.org/10.1097/01.psy.0000021952.59258.1c.

58. D'Angelo, G., Loria, A.S., Pollock, D.M., and Pollock, J.S. (2010). Endothelin activation of reactive oxygen species mediates stress-induced pressor response in Dahl salt-sensitive prehypertensive rats. Hypertension *56*, 282–289. https://doi.org/10.1161/HYPERTENSIONAHA.110.152629.

59. Fox, B.M., Becker, B.K., Loria, A.S., Hyndman, K.A., Jin, C., Clark, H., Johns, R., Yanagisawa, M., Pollock, D.M., and Pollock, J.S. (2018). Acute Pressor Response to Psychosocial Stress Is Dependent on Endothelium-Derived Endothelin-1. J. Am. Heart Assoc. *7*, e007863. https://doi.org/10.1161/JAHA.117.007863.

60. Bradley, B.P., Mogg, K., White, J., Groom, C., and de Bono, J. (1999). Attentional bias for emotional faces in generalized anxiety disorder. Br. J. Clin. Psychol. *38*, 267–278. https://doi.org/10.1348/014466599162845.

61. Stein, M.B., Simmons, A.N., Feinstein, J.S., and Paulus, M.P. (2007). Increased amygdala and insula activation during emotion processing in anxiety-prone subjects. Am. J. Psychiatry *164*, 318–327. https://doi.org/10.1176/ajp.2007.164.2.318.

62. Fonzo, G.A., Ramsawh, H.J., Flagan, T.M., Sullivan, S.G., Letamendi, A., Simmons, A.N., Paulus, M.P., and Stein, M.B. (2015). Common and disorder-specific neural responses to emotional faces in generalised anxiety, social anxiety and panic disorders. Br. J. Psychiatry *206*, 206–215. https://doi.org/10.1192/bjp.bp.114.149880.

63. Shin, L.M., Wright, C.I., Cannistraro, P.A., Wedig, M.M., McMullin, K., Martis, B., Macklin, M.L., Lasko, N.B., Cavanagh, S.R., Krangel, T.S., et al. (2005). A functional magnetic resonance imaging study of amygdala and medial prefrontal cortex responses to overtly presented fearful faces in posttraumatic stress disorder. Arch. Gen. Psychiatry *62*, 273–281. https://doi.org/10.1001/archpsyc.62.3.273.

64. Mazurski, E.J., Bond, N.W., Siddle, D.A., and Lovibond, P.F. (1996). Conditioning with facial expressions of emotion: effects of CS sex and age. Psychophysiology *33*, 416–425. https://doi.org/10.1111/j.1469-8986.1996.tb01067.x.

65. Schienle, A., Schäfer, A., Stark, R., Walter, B., and Vaitl, D. (2005). Gender differences in the processing of disgust- and fear-inducing pictures: an fMRI study. NeuroReport *16*, 277–280. https://doi.org/10.1097/00001756-200502280-00015.

66. Zilioli, S., Caldbick, E., and Watson, N.V. (2014). Testosterone reactivity to facial display of emotions in men and women. Horm. Behav. *65*, 461–468. https://doi.org/10.1016/j.yhbeh.2014.04.006.

67. Martins, J., Czamara, D., Lange, J., Dethloff, F., Binder, E.B., Turck, C.W., and Erhardt, A. (2019). Exposure-induced changes of plasma metabolome and gene expression in patients with panic disorder. Depress. Anxiety *36*, 1173–1181. https://doi.org/10.1002/da.22946.

68. Misiewicz, Z., Iurato, S., Kulesskaya, N., Salminen, L., Rodrigues, L., Maccarrone, G., Martins, J., Czamara, D., Laine, M.A., Sokolowska, E., et al. (2019). Multi-omics analysis identifies mitochondrial pathways associated with anxiety-related behavior. PLoS Genet. *15*, e1008358. https://doi.org/10.1371/journal.pgen.1008358.

69. Newman, A.M., Liu, C.L., Green, M.R., Gentles, A.J., Feng, W., Xu, Y., Hoang, C.D., Diehn, M., and Alizadeh, A.A. (2015). Robust enumeration of cell subsets from tissue expression profiles. Nat. Methods *12*, 453–457. https://doi.org/10.1038/nmeth.3337.

70. Neuenfeldt, F., Schumacher, J.C., Grieshaber-Bouyer, R., Habicht, J., Schröder-Braunstein, J., Gauss, A., Merle, U., Niesler, B., Heineken, N., Dalpke, A., et al. (2022). Inflammation induces pro-NETotic neutrophils via TNFR2 signaling. Cell Rep. *39*, 110710. https://doi.org/10.1016/j.celrep.2022.110710.

71. Daryadel, A., Yousefi, S., Troi, D., Schmid, I., Schmidt-Mende, J., Mordasini, C., Dahinden, C.A., Ziemiecki, A., and Simon, H.U. (2009). RhoH/TTF negatively regulates leukotriene production in neutrophils. J. Immunol. *182*, 6527–6532. https://doi.org/10.4049/jimmunol.0803846.

72. Alpers, G.W., Abelson, J.L., Wilhelm, F.H., and Roth, W.T. (2003). Salivary cortisol response during exposure treatment in driving phobics. Psychosom. Med. *65*, 679–687. https://doi.org/10.1097/01.psy.0000073872.85623.0c.

73. Gianferante, D., Thoma, M.V., Hanlin, L., Chen, X., Breines, J.G., Zoccola, P.M., and Rohleder, N. (2014). Post-stress rumination predicts HPA axis responses to repeated acute stress. Psychoneuroendocrinology *49*, 244–252. https://doi.org/10.1016/j.psyneuen.2014.07.021.

74. Eickhoff, S.B., Laird, A.R., Fox, P.T., Bzdok, D., and Hensel, L. (2016). Functional Segregation of the Human Dorsomedial Prefrontal Cortex. Cereb. Cortex *26*, 304–321. https://doi.org/10.1093/cercor/bhu250.

75. Maier, S., Szalkowski, A., Kamphausen, S., Perlov, E., Feige, B., Blechert, J., Philipsen, A., van Elst, L.T., Kalisch, R., and Tüscher, O. (2012). Clarifying the role of the rostral dmPFC/dACC in fear/anxiety: learning, appraisal or expression? PLoS One *7*, e50120. https://doi.org/10.1371/journal.pone.0050120.

76. Cai, R., Pan, C., Ghasemigharagoz, A., Todorov, M.I., Förstera, B., Zhao, S., Bhatia, H.S., Parra-Damas, A., Mrowka, L., Theodorou, D., et al. (2019). Panoptic imaging of transparent mice reveals whole-body neuronal projections and skull-meninges connections. Nat. Neurosci. *22*, 317–327. https://doi.org/10.1038/s41593-018-0301-3.

77. Wozny, C., and Williams, S.R. (2011). Specificity of synaptic connectivity between layer 1 inhibitory interneurons and layer 2/3 pyramidal neurons in the rat neocortex. Cereb. Cortex *21*, 1818–1826. https://doi.org/10.1093/cercor/bhq257.

78. Ferrara, N.C., Trask, S., and Rosenkranz, J.A. (2021). Maturation of amygdala inputs regulate shifts in social and fear behaviors: A substrate for developmental effects of stress. Neurosci. Biobehav. Rev. *125*, 11–25. https://doi.org/10.1016/j.neubiorev.2021.01.021.

79. Radke, S., Volman, I., Mehta, P., van Son, V., Enter, D., Sanfey, A., Toni, I., de Bruijn, E.R.A., and Roelofs, K. (2015). Testosterone biases the amygdala toward social threat approach. Sci. Adv. *1*, e1400074. https://doi.org/10.1126/sciadv.1400074.

80. van Wingen, G., Mattern, C., Verkes, R.J., Buitelaar, J., and Fernández, G. (2010). Testosterone reduces amygdala-orbitofrontal cortex coupling. Psychoneuroendocrinology *35*, 105–113. https://doi.org/10.1016/j.psyneuen.2009.09.007.

81. Pearlstein, T.B., Frank, E., Rivera-Tovar, A., Thoft, J.S., Jacobs, E., and Mieczkowski, T.A. (1990). Prevalence of axis I and axis II disorders in women with late luteal phase dysphoric disorder. J. Affect. Disord. *20*, 129–134. https://doi.org/10.1016/0165-0327(90)90126-s.

82. Phillips, N., Dennerstein, L., and Farish, S. (1996). Psychological morbidity in obstetric-gynaecology patients: testing the need for expanded psychiatry services in obstetric-gynaecology facilities. Aust. N. Z. J. Psychiatry *30*, 74–81. https://doi.org/10.3109/00048679609076074.

83. Wagels, L., Radke, S., Goerlich, K.S., Habel, U., and Votinov, M. (2017). Exogenous testosterone decreases men's personal distance in a social threat context. Horm. Behav. *90*, 75–83. https://doi.org/10.1016/j.yhbeh.2017.03.001.

84. Schaller, M., Miller, G.E., Gervais, W.M., Yager, S., and Chen, E. (2010). Mere visual perception of other people's disease symptoms facilitates a more aggressive immune response. Psychol. Sci. *21*, 649–652. https://doi.org/10.1177/0956797610368064.

85. Michopoulos, V., Powers, A., Gillespie, C.F., Ressler, K.J., and Jovanovic, T. (2017). Inflammation in Fear- and Anxiety-Based Disorders: PTSD, GAD, and Beyond. Neuropsychopharmacology *42*, 254–270. https://doi.org/10.1038/npp.2016.146.

86. Schwartz, M., Abellanas, M.A., Tsitsou-Kampeli, A., and Suzzi, S. (2022). The brain-immune ecosystem: implications for immunotherapy in defeating neurodegenerative diseases. Neuron *110*, 3421–3424. https://doi.org/10.1016/j.neuron.2022.09.007.

87. Love, M.I., Huber, W., and Anders, S. (2014). Moderated estimation of fold change and dispersion for RNA-seq data with DESeq2. Genome Biol. *15*, 550. https://doi.org/10.1186/s13059-014-0550-8.

88. Hänzelmann, S., Castelo, R., and Guinney, J. (2013). GSVA: gene set variation analysis for microarray and RNA-seq data. BMC Bioinformatics *14*, 7. https://doi.org/10.1186/1471-2105-14-7.

89. Xu, H., Liu, L., Tian, Y., Wang, J., Li, J., Zheng, J., Zhao, H., He, M., Xu, T.L., Duan, S., et al. (2019). A Disinhibitory Microcircuit Mediates Conditioned Social Fear in the Prefrontal Cortex. Neuron *102*, 668–682.e5. https://doi.org/10.1016/j.neuron.2019.02.026.

90. Chadwick, J.W., Fine, N., Khoury, W., Tasevski, N., Sun, C.X., Boroumand, P., Klip, A., and Glogauer, M. (2021). Tissue-specific murine neutrophil activation states in health and inflammation. J. Leukoc. Biol. *110*, 187–195. https://doi.org/10.1002/JLB.4AB1020-248RRR.

91. Ren, C., Yuan, Q., Braun, M., Zhang, X., Petri, B., Zhang, J., Kim, D., Guez-Haddad, J., Xue, W., Pan, W., et al. (2019). Leukocyte Cytoskeleton Polarization Is Initiated by Plasma Membrane Curvature from Cell Attachment. Dev. Cell *49*, 206–219.e7. https://doi.org/10.1016/j.devcel.2019.02.023.

92. Christenson, K., Björkman, L., Tängemo, C., and Bylund, J. (2008). Serum amyloid A inhibits apoptosis of human neutrophils via a P2X7-sensitive pathway independent of formyl peptide receptor-like 1. J. Leukoc. Biol. *83*, 139–148. https://doi.org/10.1189/jlb.0507276.

93. Roth, T.L., Nayak, D., Atanasijevic, T., Koretsky, A.P., Latour, L.L., and McGavern, D.B. (2014). Transcranial amelioration of inflammation and cell death after brain injury. Nature *505*, 223–228. https://doi.org/10.1038/nature12808.

94. Jin, H.J., Kim, J., and Yu, J. (2013). Androgen receptor genomic regulation. Transl. Androl. Urol. *2*, 157–177. https://doi.org/10.3978/j.issn.2223-4683.2013.09.01.

95. Bolton, E.C., So, A.Y., Chaivorapol, C., Haqq, C.M., Li, H., and Yamamoto, K.R. (2007). Cell- and gene-specific regulation of primary target genes by the androgen receptor. Genes Dev. *21*, 2005–2017. https://doi.org/10.1101/gad.1564207.

96. Arloth, J., Bogdan, R., Weber, P., Frishman, G., Menke, A., Wagner, K.V., Balsevich, G., Schmidt, M.V., Karbalai, N., Czamara, D., et al. (2015). Genetic Differences in the Immediate Transcriptome Response to Stress Predict Risk-Related Brain Function and Psychiatric Disorders. Neuron *86*, 1189–1202. https://doi.org/10.1016/j.neuron.2015.05.034.

97. Moore, S.R., Halldorsdottir, T., Martins, J., Lucae, S., Müller-Myhsok, B., Müller, N.S., Piechaczek, C., Feldmann, L., Freisleder, F.J., Greimel, E., et al. (2021). Sex differences in the genetic regulation of the blood transcriptome response to glucocorticoid receptor activation. Transl. Psychiatry *11*, 632. https://doi.org/10.1038/s41398-021-01756-2.

98. Menke, A., Arloth, J., Pütz, B., Weber, P., Klengel, T., Mehta, D., Gonik, M., Rex-Haffner, M., Rubel, J., Uhr, M., et al. (2012). Dexamethasone stimulated gene expression in peripheral blood is a sensitive marker for glucocorticoid receptor resistance in depressed patients. Neuropsychopharmacology *37*, 1455–1464. https://doi.org/10.1038/npp.2011.331.

99. Breen, M.S., Bierer, L.M., Daskalakis, N.P., Bader, H.N., Makotkine, I., Chattopadhyay, M., Xu, C., Buxbaum Grice, A., Tocheva, A.S., Flory, J.D., et al. (2019). Differential transcriptional response following glucocorticoid activation in cultured blood immune cells: a novel approach to PTSD biomarker development. Transl. Psychiatry *9*, 201. https://doi.org/10.1038/s41398-019-0539-x.

Please cite this article in press as: Wu et al., Meningeal neutrophil immune signaling influences behavioral adaptation following threat, Neuron (2024), https://doi.org/10.1016/j.neuron.2024.10.018

STAR★METHODS

KEY RESOURCES TABLE

REAGENT or RESOURCE	SOURCE	IDENTIFIER
Antibodies		
Anti-mouse-CD3-FITC	BioLegend	Cat# 100204; RRID: AB_312661
Anti-mouse-CD45-FITC	BioLegend	Cat# 103108; RRID: AB_312973
Anti-mouse-CD45-APC-Cy7	BD Biosciences	Cat# 557659; RRID: AB_396774
Anti-mouse-Ly6G-PE	BD Biosciences	Cat# 551461; RRID: AB_394208
Anti-mouse/human-CD11b-APC	BioLegend	Cat# 101212; RRID: AB_312795
Anti-mouse-IL-17A-APC	BioLegend	Cat# 506916; RRID: AB_536018
Anti-mouse-IFN-γ-BV421	BioLegend	Cat# 505830; RRID: AB_2563105
Anti-mouse-CD177-Alexa Fluor 647	BD Biosciences	Cat# 566599; RRID: AB_2869790
Anti-mouse-ICAM-1-APC	BD Biosciences	Cat# 561605; RRID: AB_10896297
Anti-mouse FcR (CD16/CD32)	BD Biosciences	Cat# 553141; RRID: AB_394656
*InVivo*MAb anti-mouse Ly6G	BioXCell	Cat# BE0075-1; RRID: AB_1107721
*InVivo*MAb rat anti-IgG2a	BioXCell	Cat# BE0089; RRID: AB_1107769
*InVivo*MAb anti-mouse IFN-γ	BioXCell	Cat# BP0055; RRID: AB_1107694
*InVivo*MAb rat anti-IgG1	BioXCell	Cat# BP0088; RRID: AB_1107775
Rabbit monoclonal anti-GAD65+GAD67	Abcam	Cat# ab183999; RRID:AB_2924196
Rabbit monoclonal anti-Gephyrin	Abcam	Cat# ab181382; RRID: AB_2890627
Rabbit monoclonal anti-β-actin	Sigma-Aldrich	Cat# A5441; RRID: AB_476744
Rabbit monoclonal anti-c-Fos	Cell Signaling Technology	Cat# 2250; RRID: AB_2247211
Goat anti-rabbit IgG (H+L) secondary antibody, HRP	Thermo Fisher	Cat# 65-6120; RRID: AB_2533967
Goat anti-rabbit IgG (H+L) cross-adsorbed secondary antibody, Alexa Fluor 488	Thermo Fisher	Cat# A-11008; RRID: AB_143165
Bacterial and virus strains		
AAV2/9-CaMKIIα-GCaMP6s-WPRE	Obio Technology	Cat# H11236
AAV2/9-Gad1-hM3D(Gq)-mCherry-WPRE	Obio Technology	Cat# H15962
AAV2/9-Gad1-hM4D(Gi)-mCherry-WPRE	Obio Technology	Cat# H15968
AAV2/9-Gad1-MCS-mCherry-3×Flag-WPRE	Obio Technology	Cat# H2792
Chemicals, peptides, and recombinant proteins		
Percoll	Cytiva	Cat# 17089101
Phorbol 12-myristate 13-acetate (PMA)	Sigma-Aldrich	Cat# P8139
Luminol	TCI	Cat# A5301
Lipopolysaccharide (LPS)	Sigma-Aldrich	Cat# L2630
Testosterone enanthate	Absin	Cat# abs47034289
Testosterone	Sigma-Aldrich	Cat# T1500
DAPI	Abcam	Cat# ab228544
2-methyl-2-thiazoline	Aladdin	Cat# M103076
Clozapine-N-oxide (CNO)	MCE	Cat# HY-17366
Endothelin 1 (human, porcine)	R&D system	Cat# 1160
Recombinant Murine GM-CSF	PeproTech	Cat# 315-03
Recombinant Murine IFN-γ	PeproTech	Cat# 315-05
Recombinant Murine IL-4	PeproTech	Cat# 214-14
eBioscience Cell stimulation Kit	Thermo Fisher	Cat# 00-4975-93
eBioscience Foxp3/Transcription Factor Staining Buffer Set	Thermo Fisher	Cat# 00-5523-00
Salts for aCSF, NMDG solution, intracellular solution	Sigma-Aldrich	N/A

(*Continued on next page*)

Please cite this article in press as: Wu et al., Meningeal neutrophil immune signaling influences behavioral adaptation following threat, Neuron (2024), https://doi.org/10.1016/j.neuron.2024.10.018

Continued

REAGENT or RESOURCE	SOURCE	IDENTIFIER
DMSO	Solarbio	Cat# D8371
OCT compound	Thermo Fisher	Cat# NEG-50
PBS	Cytiva	Cat# SH30256
D-Hanks	Solarbio	Cat# H1045
Hepes	Solarbio	Cat# H1095
BSA	Solarbio	Cat# A8020
FBS	Sigma-Aldrich	Cat# F8318
RPMI Medium 1640	Solarbio	Cat# 31800
Critical commercial assays		
FITC Annexin V Apoptosis Detection Kit with 7-AAD	BioLegend	Cat# 640922
MojoSort Mouse CD3 T Cell Isolation Kit	BioLegend	Cat# 480024
Testosterone Assay Kit	R&D system	Cat# KEG010
BCA Protein Assay Kit	Thermo Fisher	Cat# 23227
Deposited data		
Bulk RNA-sequencing data generated from meningeal neutrophils	This paper	GSE276662
Membrane proteome data of human neutrophils	Uriarte et al.[29]	https://doi.org/10.4049/jimmunol.180.8.5575
Gene expression data for human fear exposure	Misiewicz et al.[68]	GSE119995
Experimental models: Organisms/strains		
Mouse: B6. WT	Charles River	N/A
Mouse: B6.*Cd177*$^{-/-}$	GemPharmatech	T012005
Software and algorithms		
Graphpad Prism v9	GraphPad	https://www.graphpad.com/; RRID: SCR_002798
ANY-maze	Stoelting	http://www.anymaze.co.uk/index.htm
FlowJo v10	BD Biosciences	https://www.flowjo.com/
PatchMaster	HEKA Elektronik	https://www.heka.com/
pClamp	Molecular Devices	https://www.moleculardevices.com/
Mini analysis 6.0.3	Synaptosoft	https://www.synaptosoft.com/
LAS X	Leica Microsystems	https://www.leica-microsystems.com/
Fiji (ImageJ)	https://fiji.sc	https://fiji.sc; RRID: SCR_002285
R	The R Foundation	https://www.r-project.org
DESeq2	Love et al.[87]	https://bioconductor.org/packages/release/bioc/html/DESeq2.html
GSVA v1.40.1	Hänzelmann et al.[88]	http://bioconductor.org
CIBERSORT	Newman et al.[69]	https://cibersortx.stanford.edu/
Metascape	Metascape.org	https://metascape.org; RRID:SCR_016620

EXPERIMENTAL MODEL AND STUDY PARTICIPANT DETAILS

Mice

Adult (over 2 months old) wild-type C57BL/6 mice or Cd177-deficient mice were used for experiments. In all experiments, mice were age-matched. Littermate controls were used in all genetic deletion studies. Mice of both sexes were used to identify potential sex differences, and analyses based on sex can be found in Table S3. Mice were maintained under SPF conditions on a 12 h light-dark cycle, and provided food and water ad libitum. All behavioral procedures were performed during the dark cycle. All procedures were performed in accordance with the Chongqing Science and Technology Commission guidelines for animal research and approved by the Children's Hospital of Chongqing Medical University Animal Care Committee. Every effort was made to minimize the number of animals used and their suffering.

Please cite this article in press as: Wu et al., Meningeal neutrophil immune signaling influences behavioral adaptation following threat, Neuron (2024), https://doi.org/10.1016/j.neuron.2024.10.018

METHOD DETAILS

Threat conditioning

The socially cued fear (threat) conditioning paradigm was modified from previously described procedures.[89] Prior to conditioning, mice were individually housed for 1 week to enhance social motivation, and they remained individually housed throughout the entire process. All animals were habituated to the operant environment for 3 d before fear conditioning began. Mice were placed into a sound-attenuating shock chamber (32×32×40 cm) with white light illumination, containing two identical diagonally placed empty wire cups. After 2 min of habituation, an unfamiliar conspecific of the same sex was then placed into one of the cups and the experimental mice were allowed to explore freely for 2 min. During conditioning, the occurrence of socially motivated behaviors co-terminating with a 0.8 mA, 1 sec foot-shock delivered through grid floors. The behavior is pre-defined to occur in three types sequentially: the first involves direct contact, i.e. nose-to-nose sniffing; the second and third types involve entering a certain range (without direct contact) where the social target is located, indicating an attempt to approach. Mice were exposed to a total of 3 behavior foot-shock pairings. The behavior of mice was observed through a video system and electric shocks were delivered manually. The interval between foot-shocks depends on the latency period of mouse socially motivated behaviors. All mice received foot-shocks at intervals not exceeding 3 min. The majority of mice did not approach the social target for at least 5 min after the final foot-shock. 5 min after the last pairing ended, the social targets were removed and the mice continued to remain in the conditioning chamber for 3 min before returning to the home cage. Mice generated through the above methods exhibited robust social avoidance characteristics.

Object-cued fear conditioning is designed to train mice to associate inanimate object cues with threats. All animals were habituated to the operant environment for 3 d before fear conditioning began. Mice were placed into a sound-attenuating shock chamber with white light illumination and allowed to freely explore the environment for 2 min. After the environmental exploration, a neutral object (plastic ball) was placed in one of the corners of the ground and the mice were allowed to explore freely again for 2 min. After neutral object exploration, a new object (LEGO block) was placed in the opposite corner away from the mice. Once the mice explored the new object (sniff), they received a foot-shock (0.8 mA, 1 sec). Consistent with SFC, in subsequent pairings, mice received a foot-shock once they enter within a certain range of the new object position. The mice underwent 3 pairings, with intervals between foot shocks not exceeding 3 min, and the majority of mice did not approach the new object for at least 5 min after the final pairing. 5 min after the last pairing ended, the new objects were removed and the mice continued to remain in the conditioning chamber for 3 min before returning to the home cage. Mice remained individually housed throughout all procedures.

For classic acoustically cued fear conditioning, mice were placed into a sound-attenuating shock chamber with white light illumination. Mice were conditioned with 3 presentations (at an average interval of 60 s) of tones (CS: 3 kHz, continuous 30 sec, 70 dB) that were co-terminated with foot-shocks (US: 0.8 mA, 1 sec). After the last tone-shock pairing, mice remained in the shock chamber for 1 min before returning to their home cages. Mice remained individually housed throughout all procedures.

Threat exposure

For exposure to socially cued threat, conditioned mice were placed in a new home cage (29×18×16 cm) lined with a thin layer of bedding, then sequentially exposed to 5 novel conspecifics of the same sex for 3 min each (at an average interval of 3 min). The conspecifics were confined within wire cups placed on the short side of the home cage. Controls were exposed to empty wire cups only. For exposure to object-cued threat, the procedure was the same as above, but the objects (LEGO block) paired during conditioning were placed on one side of the home cage, and controls were exposed to neutral object cues (plastic ball). For exposure to acoustically cued threat, conditioned mice were placed in a new context (context B; solid plastic floor, black walls and dim lighting) that was different from that during conditioning (context A). After 2 min of habituation, mice were exposed to 15 presentations of the CS (at an average interval of 30 s) in the absence of the US.

Cell isolation

Mice were lethally sedated and perfused with ice-cold phosphate buffered saline (PBS). Before perfusion, peripheral blood was collected transcardially with heparin, and RBCs were lysed with RBC lysis buffer. Cells of the cranial dura were isolated by mechanical dissociation.[17] In contrast to enzymatic dissociation, mechanical dissociation was also shown to have no effect on neutrophil surface marker levels.[90] After perfusion, the mouse skull cap was removed and the dura was carefully peeled off using fine forceps. The isolated dura mater was cut into small pieces in 3.5-mm cell culture dishes containing 10% FBS in ice-cold RPMI-1640, and gently pressed through a 70-μm cell strainer using a sterile plastic plunger to obtain a single-cell suspension. For neutrophil preparation, bone marrow cells were flushed from the bone marrow cavity with Hanks-1 buffer (D-Hanks + 0.5% BSA + 10 mM Hepes) as previously described.[91] After RBCs lysis, a discontinuous Percoll density gradient centrifugation was performed. Neutrophils were collected from the bands between 81% and 60% of Percoll.

Flow cytometry

Cells were diluted to 1-2 × 10^6/100 μL and incubated with purified rat anti-mouse CD16/CD32 antibody in staining buffer (1× PBS contained 2% FBS). Cell surface antigens were stained with the fluorochrome-conjugated antibodies. For intracellular staining of cytokines, cells were stimulated with phorbol 12-myristate 13-acetate (PMA) plus ionomycin, and Brefeldin A (from eBioscience Cell stimulation Kit) for 4.5 h. At the end of stimulation, cells were fixed and stained using the intracellular fixation and permeabilization

Please cite this article in press as: Wu et al., Meningeal neutrophil immune signaling influences behavioral adaptation following threat, Neuron (2024), https://doi.org/10.1016/j.neuron.2024.10.018

kit (eBioscience Foxp3/Transcription Factor Staining Buffer Set) according to the manufacturer's instructions. Stained cells were analyzed on Meet NL-CLC flow cytometer (Cytek Biosciences) or Guava easyCyte Systerm (Luminex Corporation) or CytoFLEX (Beckman Coulter). The data were analyzed using FlowJo software.

Neutrophil ROS assays

Mouse dural cells were collected and neutrophils (MNs) were isolated. Each sample was pooled from 2 mice in the same experimental group. For measurement of total cellular ROS generation, neutrophils were incubated with the reaction buffer (HBSS with Ca^{2+} and Mg^{2+} containing 0.25% BSA, 10 mM luminol, and 100 U/mL HRP), followed by 0.2 mM PMA (Sigma-Aldrich) stimulation. Chemiluminescence was read continuously in a plate reader (Tecan).

Neutrophil survival analysis

Isolated mouse MNs were cultured for 3 h in the presence of 100 ng/mL LPS (0111:B4; Sigma-Aldrich). After 3 h, the cells were washed and the cell viability and cell death of the MNs were detected by fluorescein-labeled Annexin V antibody and 7-aminoactinomycin D (7-AAD) double staining.[92] Viable cells (Annexin V negative/7-AAD negative), early-apoptotic cells (Annexin V positive/7-AAD negative), late-apoptotic and early necrotic cells (Annexin V positive/7-AAD positive).

Depletion of MNs

For neutrophil depletion, 100 μg of anti-Ly6G (clone 1A8; Bio X cell) or rat anti-IgG2a (clone 2A3; Bio X cell) for control in 200 μL saline was injected into mice intraperitoneally 2 d before SFC and on the day of SFC. Depletion efficiency of MNs was detected 1 d after final injection by gating $CD45^+$ SSC^{high} $CD11b^+$ cells.

Bulk RNA sequencing

Transcriptional differences in MNs from male and female mice post-exposure were determined using RNA sequencing analysis by Bioprofile (Shanghai, China). The mRNA possessing a polyA structure was purified from the total RNA with the aid of Oligo (dT) beads. After fragmentation took place, the first strand of cDNA was synthesized by employing random hexamer primers and reverse transcriptase with RNA serving as the template, and the first strand cDNA was utilized as the template for the synthesis of the second strand cDNA. After the library was constructed, paired-end sequencing of these libraries was carried out by means of Next-Generation sequencing (NGS) technology based on the Illumina sequencing platform. The raw reads were filtered, and all subsequent downstream analyses were conducted on high-quality clean data. The DEseq2 algorithm was used to determine differentially expressed genes. Pathway enrichment analysis was performed using Metascape web-based tools.

Cranial bone flap transplantation

Cranial bone flap transplantation was performed as previously described.[33] Mice were placed on a 37°C heating pad under 1.5% isoflurane anesthesia. The head of Cd177-deficient mouse was shaved, and a median skin incision was made to expose the skull. The skull of Cd177-deficient mice was thinned with an electric drill until the bone flap was sufficiently freed from the surrounding skull and epidural space. Sufficient artificial CSF (aCSF) irrigation was used during skull thinning to avoid hyperthermia and adhesion of the dura mater to the inner surface of the skull, which may cause tearing of the dura mater during subsequent skull removal. The skull was ground sufficiently until the bone flap was floating. Fine forceps tips were used to lift the bone flap to form a cranial window. Simultaneously, sex- and age-matched WT donor mice were lethally sedated, decapitated, and calvaria removed. The donor skull was scissored to create a bone flap of similar size and location to the recipient's cranial window. The meninges of the donor bone flap were stripped and placed over the recipient cranial window. After transplantation, the donor bone flap was fixed with cyanoacrylate glue. After the skin was sutured, the mice were placed on a heating pad to recover. The state of the mice was observed every day, and those with poor state or poor healing of the surgical window were euthanized and no follow-up experiments were performed.

Cranial bone marrow transplantation

Eight-week-old Cd177-deficient mice were anesthetized with a dose of 100 mg kg^{-1} ketamine and 10 mg kg^{-1} xylazine administered by i.p. injection. Mice were inserted into a 1-inch-thick lead shield leaving only the head exposed. Each mouse received 9.5 Gy of gamma irradiation. Immediately after irradiation, Cd177-deficient mice were reconstituted with 2×10^6 WT bone marrow cells injected intravenously into the orbital venous plexus. After at least 4 weeks of recovery, mice were subjected to behavioral manipulation.

Cranial dura delivery

Cranial dura delivery of GM-CSF was performed similar to that previously described.[33,93] Briefly, after the last social extinction training session, mice were placed on a 37°C heating pad under 1.5% isoflurane anesthesia. The head of the mouse was shaved, and a median skin incision was made to expose the skull. Immediately afterwards, using the tip of an electric drill, the skull was carefully thinned at 4 locations near the bregma and lambda on the top of the skull until the dura mater layer was exposed. During this period, if the dura mater or brain was damaged during drilling, the mice were sacrificed and not used in subsequent experiments. 1-μL of 500 μg/mL GM-CSF or saline was applied to each cranial hole for 5 min. After the skin was sutured, the mice were placed on a heating pad to recover.

Please cite this article in press as: Wu et al., Meningeal neutrophil immune signaling influences behavioral adaptation following threat, Neuron (2024), https://doi.org/10.1016/j.neuron.2024.10.018

Social approach tests

Social approach test was conducted in a three-chambered arena constructed of gray translucent acrylic (60×40×30 cm). In each of the left and right chambers, there was a transparent, windowed cylindrical cup. The mice were first allowed to freely explore all chambers for 5 min to habituate. During the testing phase, mice were initially confined to the central chamber. A stranger conspecific of the same sex was placed into one of the cups. Immediately afterwards, mice were free to explore the three chambers for 5 min. Between two tests, the chamber was cleaned with 70% ethanol in water to remove odors. All behavioral tests were performed in dim light. ANY-Maze video tracking system (Stoelting) was used to automatically identify the movement trajectories of all tested mice and generate heatmaps. Approach (%) and avoidance (%) were defined by the ratio of the time in the chamber with the stranger mouse and the time in the chamber with the empty cage to the total time of the test, respectively.

Open field

Mice were transferred to the testing room 1 h before the start of the experiment. Mice were placed in a grey translucent acrylic arena (40×40 cm) with dim lighting. Mice were allowed to explore freely for 10 min. The behavior of the mice was tracked using the ANY-Maze video tracking system (Stoelting) and the time spent in the center (20×20 cm) was recorded.

Elevated plus maze

Mice were transferred to the testing room 1 h before the start of the experiment. The plus maze consisted of 4 arms (2 open without walls and 2 enclosed by 15-cm-high walls) that were 30 cm long and 5 cm wide. The maze was elevated 75 cm off the floor. Mice were placed into the center hub with dim lighting and allowed to explore the plus maze for 5 min. ANY-Maze video tracking system (Stoelting) was used to quantify the time spent in each arm and the number of entries.

Predator odor exposure

The fox anogenital product (2-methyl-2-thiazoline 2-MT) as an ecologically relevant aversive stimulus can evoke physical avoidance in mice. On the test day, mice were transferred to the testing room and placed in a new home cage (29×18×16 cm). 200 μL of 2-MT dilution (1/500) was dropped onto circular filter paper affixed above the cap of the 50-mL centrifuge tube. The tube cap was fixed to the side of the cage. Mice were allowed to explore freely for 5 min. At the end of each test, the filter paper was removed and 70% ethanolic water was used to clean the chamber to remove odors. Avoidance behavior is the amount of time the animals spent inside the far region (18×5 cm).

Viruses

AAV2/9-CaMKIIα-GCaMP6s, AAV2/9-Gad1-hM3D(Gq)-mCherry, AAV2/9-Gad1-hM4D(Gi)-mCherry, and AAV2/9-Gad1-MCS-mCherry-3×Flag were purchased from Obio Technology Co. (Shanghai, China). All AAV titers ranged from 3-5×10^{12} genomic copies per mL.

Stereotaxic surgery

For Stereotaxic surgery, mice (8-12 weeks) were anesthetized with 1.5% isoflurane. Viruses were bilaterally or ipsilaterally injected by a 32G metal needle connected to a hamilton syringe which mounted on a microinjection pump (RWD). To infect PrL neurons with virus, AAV2/9-CaMKIIα-GCaMP6s, AAV2/9-Gad1-hM3D(Gq)-mCherry, AAV2/9-Gad1-hM4D(Gi)-mCherry, or AAV2/9-Gad1-MCS-mCherry-3×Flag was injected into PrL of mice (700 nL/site; A/P: 2.80 mm, M/L: ±0.20 mm, D/L: -1.30 mm). For fiber photometry, an optic fiber patch cord (200-μm diameter, 0.37 NA) was unilaterally implanted into the virus injection area in the PrL. The fiber was implanted 200 μm above the virus injection site. The fiber was secured to the skull using dental cement and a small screw.

Fiber photometry

Fiber photometry was used for recording of the activity of glutamatergic neural populations within the PrL by expressing a genetically encoded Ca^{2+} indicator and implanting an optic fiber. In the fiber photometry system (ThinkerTech), a laser beam initially directed from a 488-nm laser (OBIS 488LS; Coherent) was reflected by a dichroic mirror (MD498; Thorlabs), focused by an objective lens (0.3 NA; Olympus). The patch cord was coupled with a free optic fiber, and GCaMP6s fluorescence was collected with an optical commutator (Doris Lenses). Mice were habituated with fiber in a customized chamber (25×20×30 cm). For SC recall, each mouse was exposed to a single 60-sec SC presentation after a 5-min habituation period, only once. For predator odor stimulation, in a single test, each mouse was exposed to 3 presentations of odor, each lasting 30 sec, with intervals randomly ranging from 60 to 120 sec. ΔF/F was calculated post hoc using the formula: ΔF/F=F-F1/F1-F0 for the whole experimental time, where F0 and F1 represent the values of GCaMPs signals before and after patch cord connection to mice at the beginning of the experiment, respectively. Area under the curve (AUC) was used to analyze the data.

Chemogenetic manipulation

For chemogenetic activation or inhibition of GABAergic neurons in the PrL, AAV2/9-Gad1-hM3D(Gq)-mCherry and AAV2/9-Gad1-hM4D(Gi)-mCherry were injected bilaterally into the PrL of male WT and Cd177-deficient mice, respectively. The SFC procedure was performed 4 weeks after AAV injection. CNO (1 mg/kg dissolved in saline; MCE) was delivered intraperitoneally 1 h before

Please cite this article in press as: Wu et al., Meningeal neutrophil immune signaling influences behavioral adaptation following threat, Neuron (2024), https://doi.org/10.1016/j.neuron.2024.10.018

post-test to assess the effect of GABAergic neuronal activation or inhibition on the behavioral consequences mediated by IFN-γ manipulation.

Intra-cisterna magna injections

Mice were anesthetized with 1.5% isoflurane. The head of the mouse was secured in a stereotaxic frame. The skin above the cisterna magna was cleaned and sanitized with iodine and 70% ethanol before a 10-mm linear incision was made in the midline from the top of the skull to the neck (C2 vertebra). The muscle layer was dissected, and the deep muscle was gently dissected with a cotton swab to fully expose the cisterna magna. The aCSF containing antibody or cytokine was injected slowly into the cisterna magna at a rate of 2 μL/min using a hamilton syringe (coupled to a 32G needle). For IFN-γ neutralization, 2.5 μg of anti-IFN-γ (clone XMG1.2; Bio X cell) or rat anti-IgG1 (clone HRPN; Bio X cell) for isotype control in 1 μL aCSF was injected. For IFN-γ administration, recombinant murine IFN-γ (1 μL, 20 ng; Peprotech) or aCSF was injected. The syringe was left in place for 2 min to minimize CSF backflow. After the skin was sutured, the mice were placed on a heating pad to recover. Behavioral procedures were performed at least 2-3 h after recovery.

Western blotting

Synaptosomes were isolated from the mouse dmPFC using Syn-PER Synaptic Protein Extraction Reagent (Thermo Fisher) according to the manufacturer's instructions. The synaptosomal proteins were separated on 10% SDS-PAGE gels and transferred to polyvinylidene fluoride membranes (Bio-Rad). The membranes were then incubated with 5% fat-free milk in TBS contains 0.1% Tween-20 for 1 h at room temperature to block non-specific binding site. The target proteins were immunoblotted with primary antibody overnight at 4°C to anti-GAD (1:3000), anti-gephyrin (1:2000) or anti-β-actin (1:2000). On the next day, the membranes were washed and incubated with anti-mouse HRP or anti-rabbit HRP secondary antibody (1:4,000, 2 h at room temperature). The protein band was visualized in the Bio-Rad Imager. Band intensities were quantified using Fiji (NIH).

Ex vivo whole-cell electrophysiology

Mice were deeply anesthetized and perfused with 15 mL of NMDG based ice-cold cutting solution containing 92 mM NMDG, 2.5 mM KCl, 1.25 mM $NaH_2PO_4 \cdot H_2O$, 30 mM $NaHCO_3$, 20 mM HEPES, 25 mM D-glucose, 5 mM Na-ascorbate, 3 mM Na-pyruvate, 2 mM Thiourea, 12 mM NAC, 0.5 mM $CaCl_2$ and 10 mM $MgCl_2$ (with osmolarity of 295-305 mOsm/L). After decapitation, the brain was rapidly removed and immersed in ice cold NMDG buffer oxygenated with 95% O_2 and 5% CO_2. Acute coronal slices (300-400 μm) were cut on a vibratome (Leica Microsystems) and then incubated in carbogen (95% CO_2/5% O_2) NMDG buffer (35 °C) to recover for 15 min. All slices were transferred into a braincubator filled with incubation buffer containing 92 mM NaCl, 2.5 mM KCl, 1.25 mM $NaH_2PO_4 \cdot H_2O$, 30 mM $NaHCO_3$, 20 mM HEPES, 25 mM D-glucose, 5 mM Na-ascorbate, 3 mM Na-pyruvate, 2 mM Thiourea, 12 mM NAC, 2 mM $CaCl_2$ and 2 mM $MgCl_2$ (pH 7.4, 295-305 mOsm/L) for 1 h at room temperature (23-25 °C) prior to recording. Then the slices were transferred out to the flow chamber filled with bubbled recording solution including 120 mM NaCl, 2.5 mM KCl, 1.25 mM $NaH_2PO_4 \cdot H_2O$, 24 mM $NaHCO_3$, 5 mM HEPES, 12.5 mM D-glucose, 2 mM $CaCl_2$ and 2 mM $MgCl_2$ at pH 7.4, 295-305 mOsm/L. For the miniature responses, the mIPSCs were recorded at holding potential of 70 mV in buffer containing synaptic blockers (20 mM CNQX, 50 mM AP5 and 0.5 mM TTX). Borosilicate glass electrodes (4-6 MΩ) were filled with intracellular solution consisting of 140 mM CsCl, 0.15 mM $CaCl_2$, 10 mM HEPES, 4.25 mM $MgCl_2$, 0.5 mM EGTA and 4 mM K-ATP, pH 7.2-7.3 with CsOH (295-305 mOsm/L). The parameters of mIPSCs were quantified by Mini Analysis Program 6.0.3 (Synaptosoft Inc.).

Histology

To confirm DREADD-mediated neuronal activation, 1h after CNO injection, mice were lethally sedated and perfused transcardially with ice-cold PBS. Brains were removed and fixed in 4% paraformaldehyde at 4°C for 48h before dehydration, OCT-embedding, sectioning, and staining. The brain sections were fixed in 4% paraformaldehyde for 30 min at room temperature, and then washed in PBS thrice (10 min each time) and used QuickBlock Blocking Buffer for Immunol Staining (Beyotime) for 1 h. Sections were incubated overnight at 4°C with c-Fos (9F6) Rabbit mAb (Cell Signaling) followed by incubation with the corresponding fluorescent-conjugated secondary antibodies. Slides were prepared using a DAPI-containing mounting medium and imaged under a Leica DM6B microscope.

Co-culture

$CD3^+$ T-cells were purified from mouse spleen with the MojoSort Mouse CD3 T Cell Isolation Kit (BioLegend) according to the manufacturer's instructions. To generate immature monocyte-derived DCs (moDCs), we cultured isolated monocytes for 6 days in medium supplemented with IL-4 (10 ng/mL; Peprotech) and GM-CSF (20 ng/mL; Peprotech), and the medium was changed every other day. Purified mouse BM neutrophils (2×10^6) were stimulated with GM-CSF (10 ng/mL) for 30 min at 37°C to prime neutrophils.[28] Immature moDCs were stimulated with LPS (100 ng/mL) for 3h to induce maturation. Pre-stimulated neutrophils (at a neutrophil/moDC ratio of 20:1) were cultured in contact with moDC-T-cell (1:10) cocultures or added to Transwell (0.4-μm pore; Corning) in the upper chamber. After 24 h of co-culture, the cultures were collected and the proportion of IFN-γ^+ cells in $CD3^+$ T-cells was measured by flow cytometry.

Please cite this article in press as: Wu et al., Meningeal neutrophil immune signaling influences behavioral adaptation following threat, Neuron (2024), https://doi.org/10.1016/j.neuron.2024.10.018

Orchidectomy

Mice were anesthetized with 1.5% isoflurane and subjected to a midline incision in the scrotum to expose the testes. The vas deferens and testicular vessels were ligated. The testis and epididymis were removed, and the incision was closed with sutures after successful hemostasis. Sham surgery was performed similarly, with only the testes exposed, without ligation or removal. After surgery the mice were placed on a heating pad to recover. The behavioral procedures were performed 2 weeks later.

Testosterone treatment

For testosterone replacement, following the surgery, castrated or sham mice were subcutaneously injected at the end of the light-cycle with vehicle (corn oil with 2.5% DMSO) or testosterone enanthate (5 mg kg^{-1} body weight) every other day, three times a week. In experiments assessing the acute effects of testosterone, mice received a single subcutaneous injection of testosterone (1 mg kg^{-1} body weight for castrated and female mice, 10 mg kg^{-1} body weight for male mice) or vehicle (corn oil with 2.5% DMSO) immediately following the end of exposure to SCs or before the onset of restraint stress. For testosterone stimulation *in vitro*, isolated neutrophils were seeded in a 6-well dish at a density of 5×10^{6} cells/well and incubated with10^{-8} M testosterone or 10^{-10} ET-1, separately or in combination, for 1 h.

Hormone assays

Mouse serum was collected. Testosterone concentrations were measured by a commercially available ELISA kit (R&D Systems) according to the manufacturer's protocol.

Social stimuli

All experimental mice were housed individually 24 h before the start of social session. For the social intruder stimulation, mice of the same background and sex who were unfamiliar with each other were pre-designated as either residents (experimental mice) or intruders. The intruder was removed from its home cage and placed in the resident's cage for 15 min. After the 15-min interaction ended, the intruder was removed. For mating stimulation, a conspecific of the opposite sex was placed in the cage of the experimental mouse and allowed to interact for 15 min.

Restraint stress

Restraint stress was generated by placing mice into well-ventilated restraint cylinders for 15 min without squeezing. Mice were individually restrained in home cages. In some experiments, mice were given a single subcutaneous dose of testosterone immediately following the end of 15 min of restraint.

Socially paired exposure to acoustical threats

During the exposure of conditioned acoustical cues, social stimuli were given before the start of the second CS and until the end of the 15th CS. Briefly, a pre-acclimatized conspecific of the opposite sex was placed in the chamber (context B) between the first CS and the second CS until the end of the exposure. Consistent with the social paradigm, test mice were returned to context B for post-test within 3 h after exposure. For post-test, mice were exposed to 3 presentations of the CS (at an average interval of 30 s) in the absence of the US. Freezing behaviors (no movement other than breathing) were manually counted frame by frame by colleagues blinded to experimental groups. Freezing (%) was calculated by dividing the freezing time by the tone duration.

Human dataset analysis

The blood microarray dataset of human fear exposure was extracted from the GSE119995 sequences of GEO, and the difference of cell-type fraction between men and women in peripheral blood cells before and after exposure was analyzed by CIBERSORT.

In order to generate NPS, we initially obtained the upregulated DEGs in primed human neutrophils from two independent studies,[70,71] where there was relatively less intersection between the two sets of upregulated genes. As a complementary gene set, we also compiled all the genes in the MSigDB-C5 pathways related to neutrophil function and activation. The intersection of these gene sets contained 36 genes, which we refer to as human NPS. To identify the signatures of androgen-induced transcriptional activation, we obtained 1168 overlapping androgen-regulated genes from 9 independent tumor cell microarray datasets.[94] The upregulated DEGs with androgen receptor (AR)-binding domains identified and validated in an androgen stimulation study[95] in non-tumor cells were included as a complementary gene set. The 31 overlapping genes between the two gene sets serve as the gene signature for cellular response to androgen. Finally, we compiled 417 upregulated DEGs from 3 independent *in vivo* glucocorticoid receptor (GR)-stimulated blood cell transcription studies[96–98] and included 6043 upregulated DEGs identified in *ex vivo* GR-stimulated peripheral blood mononuclear cells[99] as a complementary gene set. Furthermore, 48 target genes induced by GR stimulation from Wiki Pathways Human were also included. The intersection between the gene sets yielded 46 genes regulated positively by GR. We refer to this gene set as the gene signature for cellular response to corticosteroid.

Gene Set Variation Analysis (GSVA) is a non-parametric, unsupervised method used to estimate the enrichment changes of gene sets between samples in an expression dataset.[88] We used the R Bioconductor opensource package gsva (version 1.40.1) to calculate the enrichment scores for each sample in the gene set. GSVA was run on each dataset separately.

Please cite this article in press as: Wu et al., Meningeal neutrophil immune signaling influences behavioral adaptation following threat, Neuron (2024), https://doi.org/10.1016/j.neuron.2024.10.018

QUANTIFICATION AND STATISTICAL ANALYSIS

Data are mean ± SEM. Statistical analyses were performed with GraphPad Prism 9. For comparisons across multiple groups of defensive behavior pre- and post-exposure, either 2-way or 3-way repeated-measures ANOVA was used, and Sidak multiple comparisons test was used as appropriate. For the other comparisons across multiple groups, either 1-way ANOVA or 2-way ANOVA was used to analyze data, and Tukey multiple comparisons test was used as appropriate. Direct comparisons between two groups were tested using either an unpaired t test or paired t test, where appropriate. The datasets produced and/or analyzed in this study can be obtained from the corresponding author upon reasonable request.

Sample sizes, test, statistics, and significance levels for each experiment are listed in Table S3. t-tests and post hoc comparisons: ns $p > 0.05$, *$p < 0.05$, **$p < 0.01$, ***$p < 0.001$, ****$p < 0.0001$.